Decadal changes in phytoplankton functional composition in the Eastern English Channel: upcoming major effects of climate change?

Zéline Hubert[1], Arnaud Louchart[1,2], Kévin Robache[1], Alexandre Epinoux[1], Clémentine Gallot[1,3], Vincent Cornille[1,4], Muriel Crouvoisier[1], Sébastien Monchy[1], and Luis Felipe Artigas[1]

[1]Université Littoral Côte d'Opale, Université de Lille, CNRS, IRD, UMR 8187 LOG, Laboratoire d'Océanologie et de Géosciences, F62930, Wimereux, France
[2]Netherlands Institute of Ecology (NIOO-KNAW), Department of Aquatic Ecology, Droevendaalsesteeg 10, 6708 PB Wageningen, The Netherlands
[3]Mediterranean Institute of Oceanography (MIO), Campus de Luminy, 163 Av. de Luminy, 13288 Marseille cedex 9, France
[4]Ifremer, Unité Littoral, Laboratoire Environnement et Ressources, 150 quai Gambetta, 62321 Boulogne-sur-Mer, France

Correspondence: Zéline Hubert (zeline.hubert@univ-littoral.fr) and Luis Felipe Artigas (felipe.artigas@univ-littoral.fr)

Abstract. Global change is known to exert a considerable impact on marine and coastal ecosystems, affecting various parameters such as sea surface temperature (SST), ~~rain-off~~ run-off, circulation patterns, and the availability of limiting nutrients like nitrogen, phosphorus and silicon, each influencing phytoplankton communities differently. This study is based on weekly to fortnightly *in vivo* phytoplankton observations in the French waters of the Eastern English Channel at fine spatial resolution ($\sim$ 1 km) along an inshore-offshore gradient in the Strait of Dover. Phytoplankton functional composition was addressed by automated 'pulse shape-recording' flow cytometry, coupled with analysis of environmental variables over the last decade (2012-2022). This method allows for the characterization of almost the entire phytoplankton size range (from 0.1 μm to 800 μm width) and the determination of the abundance of functional groups based on optical single-cell signals (fluorescence and scatter). We explored seasonal, spatial, and decadal dynamics in an environment strongly influenced by tides and currents. Over the past 11 years, ~~sea surface temperatures~~ SST showed an increasing trend in all stations, with nearshore waters warming faster than offshore waters (+~~1.063~~ 1.05 °C vs. +~~0.929~~ 0.93 °C). Changes in nutrient concentrations have led to imbalances in nutrient ratios (N:P:Si) ~~compared to~~ relative to ~~Redfield molar reference ratios~~ reference nutrient ratios. ~~, though a rollback (2012-2018) to balanced ratios (since 2019)~~ However, a return to balanced ratios has been observed since 2019.. Phytoplankton total abundance has also increased over the decade, with a higher contribution of small-size cells (picoeukaryotes and picocyanobacteria) and a decrease in microphytoplankton, particularly near the coast. Based on analysis of environmental parameters and phytoplankton abundance,~~The~~ the winters of 2013-2014 and 2019-2020 have been identified as shifting periods in this time series. ~~This study provides the first assessment of decadal changes of the whole phytoplankton community by an automated *in vivo* single-cell approach, which will need to be explored further in the frame of changes in trophic transfers and water quality.~~ These changes in phytoplankton community, favoring the smallest groups, could lead to a reduction in the productivity of coastal marine ecosystems, that could affect higher trophic levels as well as the entire food web.

1 Introduction

As the main primary producer of marine ecosystems, marine phytoplankton play a crucial role in structuring pelagic food webs and greatly influence biogeochemical cycles in the ocean. This polyphyletic group exhibits a wide range of sizes (from less than a micron to centimetres), shapes, single-cell or colonial forms, life stages, pigments, storage products, motility, reproductive rates and more (Simon et al., 2009). All these functional traits, especially size, will determine their involvement and performance in biogeochemical cycling (e.g. carbon fixation, nutrient uptake; Hillebrand et al., 2022), their growth rate (Marañón, 2015) as well as energy transfer efficiency ~~in higher food webs~~ to higher trophic levels (Mehner et al., 2018). The abundance, the community composition and the succession of different phytoplankton groups are rapidly regulated by environmental parameters (~~temperature~~ sea surface temperature, light availability, nutrient disponibility) and biotic interactions (Margalef, 1978; Winder and Sommer, 2012; Barton et al., 2013; Rombouts et al., 2019). Due to the rapid turnover between generations and response of communities to environmental changes, phytoplankton is used as an indicator to assess the ecological status of pelagic marine ecosystems. In the context of the Marine Strategy Framework Directive (MSFD, 2008/56/EC), phytoplankton diversity, composition and abundance are used to assess ecological status of pelagic habitats (Louchart et al., 2023a, b; Holland et al., 2023a) and to study marine eutrophication (Rombouts et al., 2019).

In addition to local pressures, climate change significantly influences environmental parameters in marine systems, leading to rising ~~temperatures~~ sea surface temperatures (SST), changes in light intensity, rainfall and river flow (Cooley et al., 2022). Coastal and shallow environments are particularly vulnerable to these changes (Cloern et al., 2016). While these global-scale modifications are already observed at regional levels, they have not yet been observed at the sub-mesoscale (Capuzzo et al., 2018). The Eastern English Channel (EEC) is a shallow marginal sea under a macrotidal regime and heavily influenced by human activity. It is an exploited ecosystem for fisheries, hosting major harbours such as Cherbourg, Le Havre, Boulogne-sur-Mer and Calais for the French coast. The EEC is subjected to an intense maritime traffic, particularly around the Strait of Pas-de-Calais - Dover, connecting the English Channel to the North Sea, which ranks as the world's second busiest strait. Furthermore, the coastline is largely covered by agricultural land, leading to potential nutrient and/or pesticide inputs into coastal waters through rainfall. In addition, the EEC coast is characterized by numerous estuaries, including the Seine, the Somme and smaller estuaries (Authie, Canche, Liane, Wimereux and Slack) until the Strait of Dover, which collectively contribute to the 'coastal flow' generating significant terrigenous inputs (Brylinski et al., 1991). Over the last 150 years, the English Channel has witnessed a rise in precipitation (Scholz et al., 2022) and a notable increase in ~~temperature~~ SST since the 1990s was observed in its Eastern part (McLean et al., 2019; Tinker et al., 2020). On the other hand, changes in nutrient concentrations were observed after implementation of the European Common Agricultural Policy (CAP), resulting into stronger phosphorus mitigation effort than nitrogen, leading to an imbalanced N:P ratio (Loebl et al., 2009; Talarmin et al., 2016; Lheureux et al., 2023). These modifications are expected to have consequences on phytoplankton communities in the EEC, affecting their abundance, composition, size, and bloom timing (Falkowski and Oliver, 2007; Sommer and Lengfellner, 2008; Winder and Sommer, 2012; Henson et al., 2018; Rombouts et al., 2019).

Previous time-series studies have revealed a decline in phytoplankton biomass in the EEC using chlorophyll *a* measurements (Lefebvre et al., 2011; Gohin et al., 2019). Over the past decade, analysis of Continuous Plankton Recorder (CPR) data has shown a change in phytoplankton composition in the North Sea, characterized by an increase in ~~small~~ diatoms and dinoflagellates (Holland et al., 2023b). In the EEC, the years between 1992 and 2007 could be categorized according to the dominance of the haptophyte *Phaeocystis globosa* or diatoms (Lefebvre et al., 2011). Previous long-term studies in the EEC, based on satellite images, chlorophyll *a*, microscopy or CPR, enable to adress some changes in phytoplankton phenology and diversity, but they neglect picophytoplankton and some nanophytoplankton. In the Western English Channel, it was shown that small phytoplankton represented 99.98% and 71% of phytoplankton abundance and biomass (McQuatters-Gollop et al., 2024) and that ~~temperature~~ SST increase can lead to changes in the structure and cell size of this community (Zohary et al., 2021). However, these compartments were overlook by microscope observations, while playing a significant role in marine ecosystems by recycling nutrients and dissolved organic matter(microbial loop), and the export of carbon to higher trophic level through zooplankton consumption. In a context of climate change, a modification in the balance between pico- and nanophytoplankton communities structure could increase the importance of microbial loop and microbial food webs, reduce carbon sequestration (respiration, carbon fixation, ocean carbon export), change the trophic pathways and *in fine* influence higher trophic levels including fisheries (Falkowski et al., 2000; Laws et al., 2000; Hillebrand et al., 2022).

In this study, we used data acquired regularly since 2012 on the full size range of phytoplankton, including picophytoplankton, addressed *in vivo* by automated 'pulse shape-recording' flow cytometry, coupled with environmental variables. Some previous studies applying this approach in the EEC were performed describing seasonal (Bonato et al., 2016) and short interannual changes (Breton et al., 2017), as well as spatial and temporal variability on oceanographic cruises (Bonato et al., 2015; Louchart et al., 2020, 2024). The aim of this study was to identify and quantify changes at sub-mesoscale and to report for the first time decadal trends on the entire phytoplankton community. ~~The approach combined high frequency compared to most reference observation networks, and high spatial resolution across all water types, from nearshore to offshore waters, in a frontal system by the Strait of Dover.~~ The approach combines relatively high frequency with high spatial resolution, complementing most reference observation networks for all types of water, from inshore to offshore, in a frontal system near the Strait of Dover. To characterize these trends and assess magnitude of phytoplankton communities change over a decade, we applied a functional community composition approach. This approach considered temporal changes in biomass, abundance and composition, relative to changes in environmental variables, from single-cell up to community levels.

2 Materials and Methods

2.1 Study area and sampling strategy

Subsurface marine samples were collected weekly to fortnightly, from February 2012 to December 2022, on board the R/V *Sepia II* (CNRS INSU-FOF) ~~R/V~~. The data set consists of 1,835 samples distributed along a longitudinal transect, over 268 sampling dates. Sampling was conducted along a nearshore-offshore transect located by the Dover Strait (EEC), known as DYPHYRAD monitoring. This transect consists of ~~9~~ nine sampling stations (Fig. 1), from R0 (50°8' N; 1°59' E) to R4 (50°8' N;

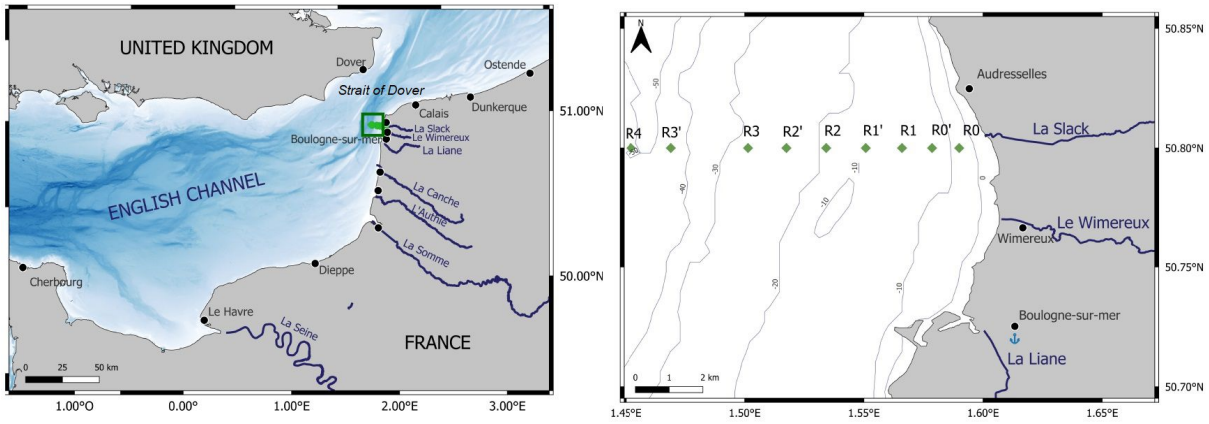

(a) Study area (b) Zoom on station locations

Figure 1. Map of the study area (a) the Eastern English Channel and (b) location of DYPHYRAD stations off the Slack River estuary by the Strait of Dover.

1°45'22 E), spaced between 0.8 kilometers to 1.7 kilometers. Stations characterized three zones (from offshore to nearshore): offshore (R4, R3, R3'), frontal (R2, R1') and nearshore (R1, R0', R0), in order to facilitate the description of spatial phenomena, according to Brylinski et al. (1991).

2.2 Environmental parameters

~~Temperature~~ Sea surface temperature (SST, °C) and salinity (S, PSU) were recorded at each sampling station sub-surface (1 to 2 meters depth) with a Conductivity Temperature Depth (CTD) probe (SBE19 + and SBE 25, SeaBird Ltd, United States). Sub-surface water layer (1 meter depth) were collected using a Niskin bottle. Dissolved inorganic nutrient concentrations (NO_2^-, NO_3^-, ~~SiO_2~~ $Si(OH)_4$ and H_3PO_4) were measured at the main sampling points (R0, R1, R2, R3, R4). Seawater samples were collected and kept cooled in the dark by placing them in a icebox with ice packs for up to 3 hours until return to the laboratory where it was frozen (-20 °C) until analysis. This nutrient preservation process is recommended when samples cannot be analyzed on the same day (Aminot and Kérouel, 2007). Nutrient concentrations were obtained using an autoanalyser (AutoAnalyzer ALLIANCE SpA, Italy and, since 2016, a AA3 HR AutoAnalyzer, SEAL Analytical GmBH, Germany), following the French coastal observation network 'Service d'Observation en Milieu Littoral' (SOMLIT) protocol (Garcia and Oriol, 2019; Breton et al., 2023). ~~Nitrogen will be referred to as the sum of nitrite (NO_2^-) and nitrate (NO_3^-).~~

2.3 Phytoplankton biomass, abundance and size

~~Phytoplankton biomass was estimated through chlorophyll *a* concentration analysis.~~ Phytoplankton biomass was approached using chlorophyll *a* concentration analysis in sub-surface waters, even though we aknowledge that there is a variability in Chl:C. Between 250 mL to 1 L of seawater were filtered on 47 mm diameter GF/F (Whatman) filters and then stored at -80 °C until

pigment analysis, after extraction on 90 % acetone at 4 °C overnight. Chlorophyll *a* and degraded pigments (phaeopigments) concentrations were measured both before and after acidification (HCl 0.2 mol L^{-1}) on a Turner Designs benchtop fluorometer (10-AU Field Fluorometer, Turner Designs Ltd, USA) following the protocol developed by Holm-Hansen et al. (1965) and the equations developed by Lorenzen (1967).

Phytoplankton functional composition was obtained from *in vivo* samples using CytoSense~~s~~ (Cytobuoy b.v., Netherlands). Over the 11 years of the time series, four cytometers were used. To ensure maximum combarability between the data from each instrument, the data were acquired using as much as possible the same protocols, then processed by the same person to maintain clustering consistency. In addition, only abundances were used, to avoid the risk of biasing the analysis by the inclusion of highly machine-dependent fluorescence. Abundances were compared on common samples when machines were changed. The flow cytometers are equipped with a blue laser (488 nm, 50 mW) to allow discrimination between phototrophic and non-phototrophic particles. Flow cytometers provide counting of particle for sizes from 0.1 to 800 μm width, to consider practically the whole phytoplankton size-range. Technical specifications for the flow cytometer can be found in previous studies using this instrument at Laboratory of Oceanology and Geosciences (LOG; Bonato et al., 2015, 2016; Louchart et al., 2024). Each sample underwent analysis using two separate protocols, each targeting specific size and optical parameters. The first protocol, referred to as the 'Pico' protocol, used a low detection threshold (around 10 mV red fluorescence), a low pump speed (5 μL s^{-1}) and a short sampling time (5 minutes). This protocol targeted cells ranging from 0.1 to 3 μm in size, characterized by low fluorescence and high abundance. The second protocol focused on nano– and microphytoplankton, using a higher detection threshold (around 25 mV red fluorescence), a high pump speed (between 10 and 13 μL s^{-1}) and a long sampling time (8 to 10 minutes).

Manual discrimination and characterization of six main Phytoplankton Functional Groups (PFGs) was performed on the basis of their size distribution, structure complexity and fluorescence signals, in accordance with the interoperable vocabulary of Thyssen et al. (2022). Cytogram analysis (biplot combining scatters or fluorescence) was performed using CytoClus 4 software (Cytobuoy b.v., Netherlands). Several of these functional groups have been previously identified in the area, including OraPicoProk (e.g. *Synechococcus* spp. type cells), RedPico (e.g. picophytoplankton), RedNano (e.g. nanophytoplankton, mainly dominated by *Phaeocystis globosa* during the spring bloom; Bonato et al., 2015, 2016; Guiselin, 2010), HsNano (e.g. coccolithophore type cells), OraNano (e.g. cryptophyte type cells), and RedMicro for microphytoplankton (Fig. 2).

For the final PFG dataset, only picoeukaryotes (RedPico) and cyanobacteria (OraPicoProk) were considered in the 'Pico' protocol. The other groups (RedNano, OraNano, HsNano and RedMicro) were classified using the 'Micro' protocol. To accurately perform phytoplankton functional group discrimination and labeling, we used 1 and 3 μm fluorescent beads (labelled with yellow and multi-fluorescence dyes, respectively; Fluospheres Carboxylate-Modified, Invitrogen, 1.0 μm, yellow-green fluorescent and Sphero brand beads, Spherotech Inc., 3.0-3.4 μm, bright intensity).

2.4 Statistical analysis

All data analysis, graphical representations and statistical analyses were carried out using R software (R-project, CRAN) version 4.3.1. The plots were produced using the 'ggplot2' package, version 3.5.0. Date management was implemented using

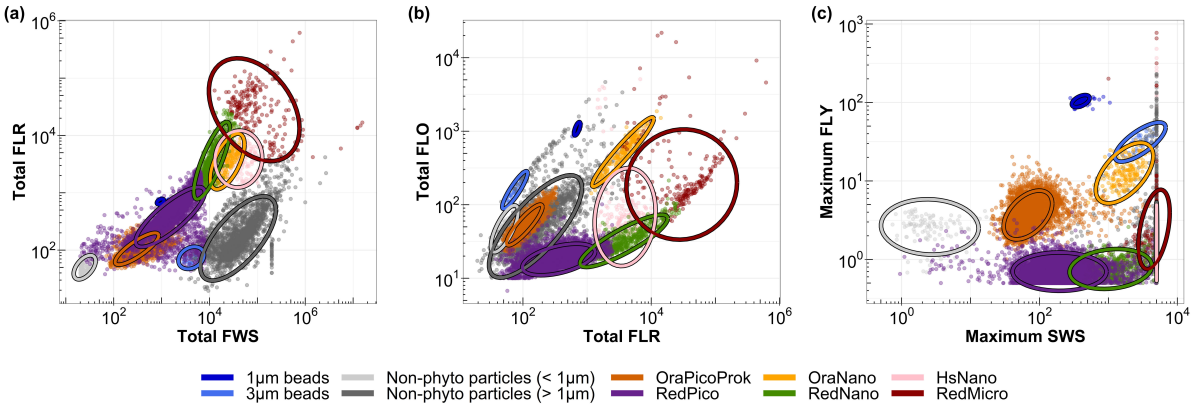

Figure 2. Cytograms of EEC used to characterize the main phytoplankton groups: (a) total red fluorescence vs total forward scatter for the discrimination of ~~picoeucaryotes~~ picoeukaryotes (RedPico), ~~nanoeucaryotes~~ nanoeukaryotes (RedNano) and ~~microeucaryotes~~ microeukaryotes (Red Micro), (b) total red fluorescence vs total orange fluorescence for the discrimination of *Synechococcus* spp. (OraPicoProk) and Cryptophytes (OraNano), (c) maximum yellow fluorescence vs maximum sideward scatter for the discrimination of *Coccolithophoridaea* (HsNano). Ellipses on the graphs are calculated from a t-distribution at 95 % confidence level, aiding in accurate delineation of the respective phytoplankton groups.

the 'lubridate' package, version 1.9.3. Multivariate statistical analyses were performed using the 'vegan' package version 2.6-4 and trend tests were performed using the 'trend' package version 1.1.6.

2.4.1 Spatial and seasonal pattern

Spatial and annual variability of environmental parameters and phytoplankton communities were investigated along the DYPHYRAD transect. Stations were not uniformly sampled due to difficult weather conditions. Thus, we applied a linear time series interpolation ~~on this station~~ at each station to fill these gaps and define regular and complete sampling intervals. The abundance data was $\log_{10}+1$ transformed in order to reduce the weight of high abundance in the analyses. Seasonal dynamics was evaluated by applying a Generalized Additive Model (GAM). This statistical model develops linear regression by considering non-linear relationships between dependent and independent variables through the use of smooth functions. In this study, GAM facilitated the exploration of variability in phytoplankton functional group abundance over time using smooth spline estimation, as shown in the following formula:

$$g(abundance) = S_0 + S(year) + \epsilon, \epsilon\ N(0, \sigma^2) \quad (1)$$

where S_0 is the intercept, S the smoothing function, ϵ the GAM regression and σ the standard deviation.

This method facilitates the modelling of non-linear relationships between the time factor and the abundance variable. We applied these GAMs individually to each PFG within every station. These relationships were created using the mgcv GAM function, without any manually imposed constraints. The smoothing of the curves corresponds to the smoothing of the GAM function in the "Smoothed conditional averages" package.

2.4.2 Spatio-temporal interaction

To assess the spatio-temporal variability of PFGs over the different years, seasons and stations included in the time series, we used PERmutational Multivariate ANalysis Of VAriance (PERMANOVA). This statistical method is particularly robust because it is non-parametric and relies on permutations in the context of the Bray-Curtis distance matrix that was used. Before conducting the analysis, we standardized abundance values using the Hellinger transformation as proposed by Legendre and Gallagher (2001) to reduce the influence of the most dominant groups while preserving the contribution of rare groups. This standardisation is often applied to abundance data, as it preserves the proportions between groups while reducing the effect of extreme values maintaining the distances between samples. The strength of PERMANOVA lies in its permutation-based testing approach, making it resilient against assumptions about data distribution. In this study, we performed 999 permutations to ensure robustness and statistical validity of the results. In the event of a significant difference within a parameter (year, season, station), a post-hoc Tukey multiple comparison test (or Tukey's Honestly Significant Difference) was performed (Tukey, 1949) to determine which of all possible pairs have a significant difference at a 95 % confidence interval.

2.4.3 Decadal changes and trends

The analysis of decadal changes and trends in time series was based on the processing of raw data, which were averaged on a monthly basis to establish a consistent and regular time interval. To analyze changes without eliminating the seasonal cycle, we have subtracted the monthly average for each year from the monthly average for the entire period under consideration.

The cumulative sums method was used to analyse trends and patterns of the time series dataset after checking the non-normality of the data with the Shapiro-Wilk test (Shapiro and Wilk, 1965). This method is particularly robust in the case of data series with gaps, noise or following a non-normal distribution (Regier et al., 2019). The cumulative sums corresponded to the successive addition of each anomaly value in a chronological order. By analysing these cumulative sums over time, we were able to define periods of below-average values (in the case of a decreasing slope) and above-average values (in the opposite case of an increasing slope; Regier et al., 2019) and deduce phases of increasing or decreasing parameters of interest. Moreover, a change in the direction of the slope can be used to identify inflexion points in the series (Regier et al., 2019).

The Mann-Kendall trend test was applied to determine the general direction of trends over time (monotonic trend; Mann, 1945; Kendall, 1948) to obtain the general sign of the slope (by adding together all the signs two by two) for each parameter. The Mann-Kendall test gives no indication of the magnitude of the trend but only its sign. This was combined with a Sen slope calculation to quantify the magnitude of change within the series (Sen, 1968). This non-parametric test was used to obtain a slope value corresponding to the median of all slopes (expressed in units per decade) in the series (in pairs). These trend tests were carried out on the whole series, analyzing trends by station in order to observe small-scale spatial variations.

2.4.4 Nutrients ~~imbalance~~ stoichiometry

Potential nutrient limitations over the last decade were identified through a diagram of Si:N:P molar ratios ~~wheere~~ where data were averaged by year. This diagram is based on the ratios Si:N = 1:1, N:P = 16:1 and Si:P = 16:1 previously described by

Redfield et al. (1963) and Brzezinski (1985). To improve visualization, the axes were transformed into $\log_{10}$ and the graph was divided into six zones, each describing a nutrient limitation as was done previously by Pannard et al. (2008), Schapira et al. (2008) and Akanmu (2018).

3 Results

3.1 Seasonal pattern along a nearshore-offshore gradient

The Generalized Additive Model (GAM) modelling environmental parameters, offered valuable insights into the transect dynamic characteristics throughout a standard year (Fig. 3). ~~Temperatures~~ SST peaked between the day 220 and day 240 (Julian day), depending on the station, preceded by minimum values between the day 30 and day 60 of the year. Spatial fluctuations in sea surface ~~temperature~~ SST were nuanced, with slight shifts between increases and decreases. In particular, nearshore waters showed greater reactivity than offshore waters, with ~~temperature~~ SST colder in winter and warmer in summer, earlier than in offshore waters. Salinity was highest in summer, showing a gradual increase from winter values and an abrupt decrease in the summer-~~fall~~ autumn transition. Salinity revealed a distinct and contrasting spatial pattern between nearshore and offshore waters, with station R0 consistently displaying lower salinity levels (from 33.10 to 34.10) compared to others stations along the transect. Salinity levels increased progressively from coastal towards offshore waters, punctuated by intermittent periods of inversion, such as those observed between day 1 and day 70 (March 11th) at station R4, where salinity fell below that of R3'. The spatial difference was less marked in summer compared to winter. Nutrient concentrations also showed a seasonal pattern, starting with high values during the first months of the year (January-February), followed by a decline in spring, before increasing again from summer to autumn-winter. ~~Silicate~~ Silicic acid (Si) showed a sharp depletion from offshore to nearshore waters with lower concentrations around day 110 (from 0.3 to 0.6 μmol L^{-1}), with a notable early increase observed at station R0 around day 200 (July, 19th) compared to a later increase in the other stations. Phosphate and ~~nitrogen~~ $[NO_2^- + NO_3^-]$ concentrations showed similar temporal dynamics, both declining in spring, later than ~~silicate~~ Si concentration, following different trends on nearshore stations. ~~Nitrogen~~ $[NO_2^- + NO_3^-]$ concentration increased from offshore to nearshore areas, and was almost depleted in late spring and summer, whereas R0 showed an slightly earlier summer-~~fall~~ autumn increase compared to offshore waters. Phosphate showed a more complex pattern, with higher phosphate concentration in nearshore station R0 in spring and an increase from day 155, earlier than the rest of the stations (increase registered from day 180 to 220).

Chlorophyll *a* concentration showed a pronounced increase early in the year reaching higher values (spring bloom; 3 to 7.5 μg L^{-1}) from day 85 to 95 in all stations and more particularly at station R0', followed by a decrease to values similar to stations R0, R1 and R1' (Fig. 4, left). A strong spatial gradient was evidenced grouping the first 4 nearshore stations, the two frontal stations (R2 and R2') and the gradient on offshore stations (R3, R3', R4). It was much more pronounced during the bloom period than during the rest of the year with the most ~~littoral~~ coastal station (R0) concentration decreasing to offshore levels from late spring. On the other hand, total abundance showed a pattern opposite to that of chlorophyll *a*, with a minimum abundance in spring and a maximum in summer (Fig. 4, right). An increase in total abundance was evidenced from spring only in the two nearshore stations R0 and R0', whereas a marked spatial pattern was observed from late spring-summer to early

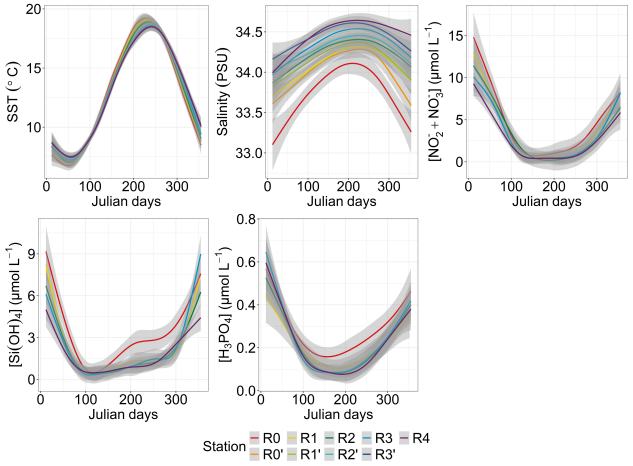

Figure 3. Seasonal and spatial variability of environmental parameters: ~~temperature~~ SST ~~(°C)~~(N=1,766), salinity ~~(PSU)~~(N=1,729), ~~nitrogen~~ $[NO_2^- + NO_3^-]$ ~~(μmol L^{-1})~~(N=1,021), ~~silicate~~ Si ~~(μmol L^{-1})~~(N=1,017) and phosphate ~~(μmol L^{-1})~~(N=1,024). The smoothed curves are modelled per Julian day using GAM.The shaded area is the confidence interval.

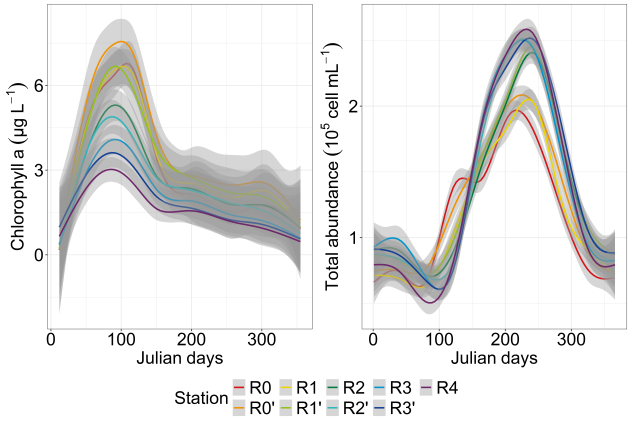

Figure 4. Seasonal and spatial variability of total phytoplankton parameters: chlorophyll *a* ~~(μg L^{-1})~~(N=1,769) and total abundance ~~(cells mL^{-1})~~(N=1,522 and N interpolated=35,712). The smoothed curves are modelled per Julian day using GAM. The shaded area is the confidence interval.

~~fall~~ autumn, with decreasing abundance from offshore waters (R4, R3, R3'), to frontal area (R2', R2, R1'), reaching the lowest cell abundance in nearshore waters (R1, R0', R0).

The GAM analysis revealed a relatively high variability across space and over time, for the six PFGs (Fig. 5). The seasonal heterogeneity was most striking across the PFGs, rather than across different water bodies, considering a single PFG. However, RedMicro and HsNano (and, to a lesser extent, RedNano in spring) presented a marked spatial heterogeneity. PFGs with phycobilins dominance (OraPicoProk and OraNano) reached their lowest abundance in spring (April-May) and their highest

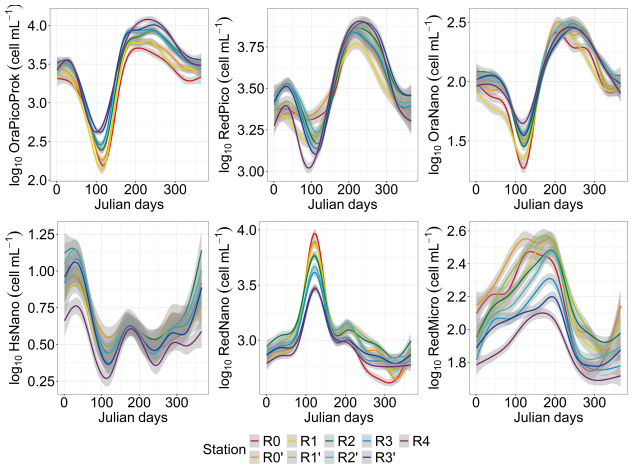

Figure 5. Seasonal and spatial variability of Phytoplankton Functional Groups abundance (N=1522 and N interpolated=35712). The smoothed curves are modelled per Julian day using GAM.The shaded area is the confidence interval.

abundance during summer- early ~~fall~~ autumn period (July-September). The abundance of these PFGs increased along the nearshore-offshore transect. On the other hand, the abundance of PFGs with chlorophyll *a* dominance (RedPico, RedNano, RedMicro and HsNano) decreased along the neashore-offshore transect. The seasonal pattern of RedPico followed those of OraPicoProk and OraNano. The seasonality of RedNano was characterised by a highest abundance in spring (April-May) and a lowest in summer with minimum values in autumn-winter. Throughout the rise and fall of the spring bloom, the RedNano group displayed almost no apparent spatiality dynamics, albeit some spatial difference considering their total abundances. During the autumn-winter period, the nearshore-offshore pattern of RedNano disappears, replaced by a different spatialization with a higher abundance in the middle of the transect, and lower abundances at the extreme stations (R0 and R4). RedMicro abundance increased from January to July before dropping. Towards the end of the year (from day 250), RedMicro abundance was the highest in stations R0' and R1'. HsNano abundance was more variable than that of any other PFG, maybe because of low occurrence of high scattering PFG in the study area (coccolithophores and thecate dinoflagellates).

3.2 Spatial and temporal interaction in the Dover Strait dynamics

Over the last decade, ~~environmental variables and phytoplankton communities significantly explained 45 % and 39 % of the respective variances~~ seasons had significantly explained 45 % and 39 % of the variances in environmental variables and phytoplankton communities (PERMANOVA p-value < 0.05) with a strong difference according to the F-statistic score (Table 1, and 2). The sampling year was the second most important factor in explaining the variance and influence on phytoplankton abundance (15 %) and on environmental variables (11 %). Finally, over the whole decade, stations location along the transect (expressed in Longitude) only explained 5 % very little of the variances for phytoplankton abundance and environmental variables. The combined factors of year and season explained 6.9 % of the variance for phytoplankton abundance groups and 9.8 % of the variance for abiotics parameters. Pairwise post-hoc tests showed that all seasons differed significantly (p-value < 0.05)

Table 1. PERMANOVA partitioning and analysis of environmental variables (~~temperature~~ SST, salinity, ~~nitrogen~~ $[NO_2^- + NO_3^-]$, phosphate, ~~silicate~~ Si) from the decadal data, based on range-transformed values and Bray–Curtis dissimilarities. Df stands for degrees of freedom, the coefficients of determination (R^2) explaining the variability of the dependent variable. The F statistic evaluates the size effect, the higher the F, the greater the variation. Bold indicates a significant effect on variability (p-value < 0.05).

Source	df	R^2	F-statistic	p-value
Year	10	0.114	26.39	**0.001**
Station	4	0.050	28.89	**0.001**
Season	3	0.448	344.70	**0.001**
Year × Station	40	0.01	0.626	0.995
Year × Season	26	0.098	8.72	**0.001**
Station × Season	12	-0.002	-0.44	1.000
Year × Station × Season	95	0.021	0.51	1.000

Table 2. PERMANOVA partitioning and analysis of phytoplankton abundance from the decadal data, based on Hellinger-transformed abundances and Bray–Curtis dissimilarities. Df stands for degrees of freedom, the coefficients of determination (R^2) explaining the variability of the dependent variable. The F statistic evaluates the size effect, the higher the F, the greater the variation. Bold indicates a significant effect on variability (p-value < 0.05)

Source	df	R^2	F-statistic	p-value
Year	10	0.150	50.48	**0.001**
Station	8	0.011	4.58	**0.001**
Season	3	0.391	437.16	**0.001**
Year × Station	80	0.009	0.38	1.000
Year × Season	27	0.070	8.66	**0.001**
Station × Season	24	0.003	0.42	1.000
Year × Station × Season	194	0.017	0.29	1.000

from one another in terms of abiotic parameters, with the exception of autumn and winter for phytoplankton communities. No significant differences were observed between stations regarding phytoplankton communities, with the exception of R0 that was significantly different from all stations for environmental parameters according to Tukey's post-hoc test (p-value < 0.05).
250 Considering the interannual variability, 2020 differed significantly from all other years (except 2015) for abiotic parameters, while for phytoplankton communities it differed from 2012 and 2017. In addition, abiotic parameters for 2015 and 2022 also differed from other years in the series (2012, 2013, 2017, 2021, 2022 and 2014, 2015, 2019, 2020 respectively). Phytoplankton communities are particularly different from 2017 onwards, with 2020 and 2021 being the most different from all other years.

3.3 Long-term variability

3.3.1 Environmental decadal evolution

Between 2012 and 2022, the sea surface waters within nearshore-offshore transect exhibited notable fluctuations in ~~temperature~~ SST, salinity, and concentration of key nutrients such as nitrite, nitrate, phosphate and ~~silicate~~ Si. These variations were analyzed as part of a global approach incorporating both cumulative sums and general trends for each parameter over time. At the beginning of the time series, the cumulative sum analysis for ~~temperature~~ SST (Fig. 6a) indicated below-average values (negative slope) influenced by starting value. Since 2014, an overall trend of ~~temperatures~~ SST increase was observed with consistently above-average ~~temperatures~~ SST (positive slope). Besides some fluctuations, raw data and decadal ~~temperatures~~ SST trend analysis corroborated this observation, revealing an overall increase ranging from +0.89 to +1.21 °C between February 2012 and December 2022 (Sen slope values, p-value < 0.05). Nearshore waters showed more pronounced warming compared to offshore waters (Table 3). Sea surface salinity (Fig. 6b) began with a phase of decline until winter 2013, increases until winter 2019 then declines again until the end of the studied period. Although trend tests failed to detect any significant trends in salinity values over the period (Table 3), all values were negative and, in line with the fluctuations observed in both raw data and cumulative sums. Regarding nutrient levels, ~~nitrogen~~ $[NO_2^- + NO_3^-]$ concentrations (Fig. 6c) displayed a 'U' shape pattern throughout the decadal period, decreasing from particularly high values during winter 2013-2014 (~~NOx~~ $[NO_2^- + NO_3^-] > 20$ μmol L^{-1}) and then increase to high values from January 2018 and in winter 2021-2022 (~~N0x~~ $[NO_2^- + NO_3^-] > 10$ μmol L^{-1}). However, a significant decrease (Mann-Kendall trend analysis) in ~~nitrogen~~ $[NO_2^- + NO_3^-]$ was observed at stations R0 and R1 (nearshore waters) during the whole period (Table 3). The cumulative sum analysis of phosphate concentrations revealed a more intricate pattern (Fig. 6d), characterized by alternating phases of increase and decrease, punctuated by peaks in winter 2015-2016 and 2019-2020. Trend analysis indicated an overall increase in phosphate concentration at nearshore stations (R0 and R1, Table 3). Cumulative sums of ~~silicate~~ Si concentration depicted a declining trend since winter 2013-2014 except during winter 2019-2020 (Fig. 6e). Raw data highlight elevated concentrations during the winter of 2019-2020. Significant increases in ~~silicate~~ Si levels were detected from R2 (frontal waters) to R4 (offshore waters) stations (Table 3). ~~The combined analysis of raw data, cumulative sums and trend tests facilitated the identification of trends and periods of change in physico-chemical variables, such as the transition between 2013 and 2014, as well as the period from 2018 to 2020.~~ The combined analysis of raw data and cumulative sums has enabled us to identifying periods of change in physico-chemical variables (according to Regier et al., 2019), such as the transition between 2013 and 2014, as well as the period from 2018 to 2020, by observing changes in slope. On the other hand, trend tests (Mann-Kendall) and slope calculations (Sen slope estimate) facilitated trend identification and quantification.

Fluctuations in nutrient concentration have implications on ~~Redfield ratios~~ nutrient ratios and in turn underline potential nutrient limitation. Consequently, phytoplankton would respond to these variations through changes in the community composition, biomass and productivity. The assessment of interannual averages across all stations was conducted to investigate annual nutrient potential limitations (Fig. 7). From 2012 to 2015, the system exhibited indications of potential phosphate limitation (Fig. 7, top part), corresponding to the elevated ~~nitrogen~~ $[NO_2^- + NO_3^-]$ values observed at the beginning of our time series

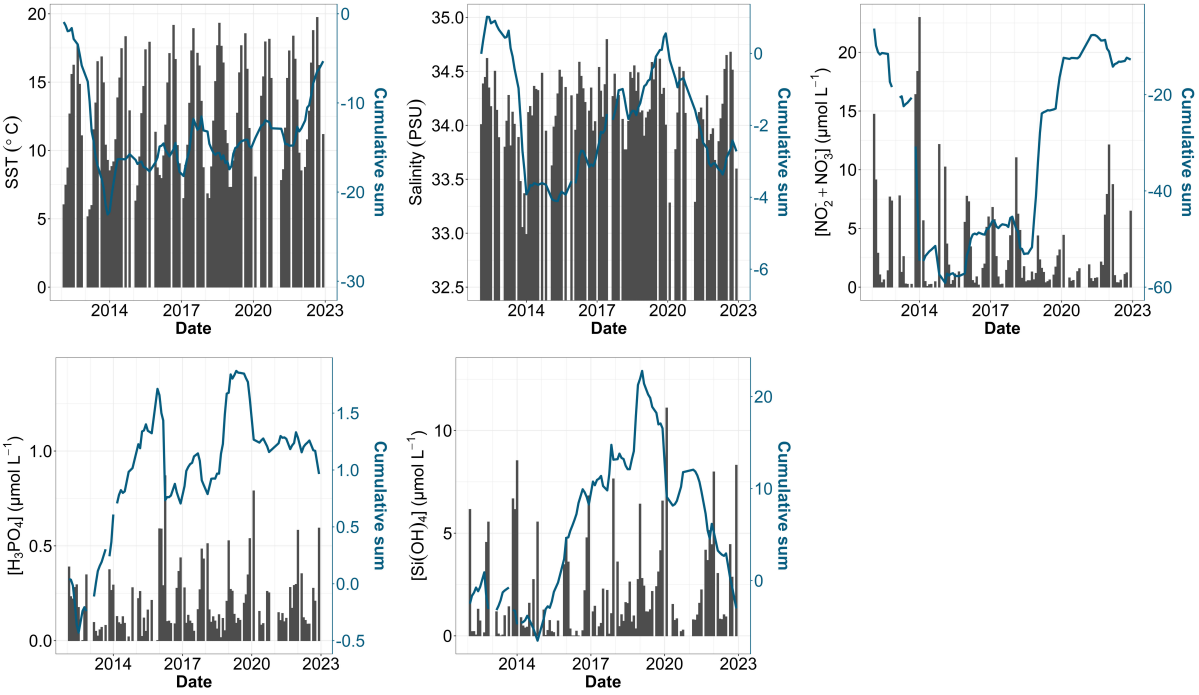

Figure 6. Time series of environmental parameters: (a) ~~temperature~~ SST, (b) salinity, (c) ~~nitrogen~~ $[NO_2^- + NO_3^-]$, (d) ~~phosphate~~ $[H_3PO_4]$ and (e) ~~silicate~~ $[Si(OH)_4]$. Bar plot represents monthly raw data for all stations combined (left y-axis). The blue lines correspond to the cumulative sum of anomalies over time (based on the difference between these monthly averages and the monthly average for the period), right y-axis).

Table 3. Trends and magnitude (slope) of change of ~~temperature~~ SST, salinity, ~~nitrogen~~ $[NO_2^- + NO_3^-]$ ~~$(NO_2 + NO_3)$~~, phosphate and ~~silicate~~ Si from Mann-Kendall test and Sen slope calculation. Bold indicates a significant trend (p-value < 0.05) over the period 2012-2022. The figures indicate the magnitude of the trend.

Parameters (Units)	R0	R0'	R1	R1'	R2	R2'	R3	R3'	R4
~~Temperature~~ SST (°C)	**+1.05**	**+1.18**	**+1.21**	**+1.01**	**+0.94**	**+0.89**	**+0.95**	+0.95	**+0.93**
Salinity (psu)	-0.15	+0.07	-0.035	-0.05	-0.05	-0.099	-0.10	-0.12	-0.07
~~Nitrogen~~ $[NO_2^- + NO_3^-]$ (μmol L^{-1})	**-1.025**	-	**-0.94**	-	-0.29	-	-0.264	-	0.127
Phosphate (μmol L^{-1})	**+0.09**	-	**+0.05**	-	+0.025	-	**0.000**	-	**-0.026**
Silicate (μmol L^{-1})	+1.21	-	+0.75	-	**+1.08**	-	**+1.38**	-	**+1.39**

(Fig. 6c). In 2016 and 2017, the ~~Redfield ratios~~ nutrient ratios shifted towards a potential ~~silicate~~ Si-limited system (Fig. 7, bottom left). Since 2019, a trend towards a potential ~~nitrogen~~ $[NO_2^- + NO_3^-]$ limitation becomes apparent. However, since 2020, the system seemed to be moving towards an equilibrium in the N:P:Si ratio. These shift periods aligned with the break-

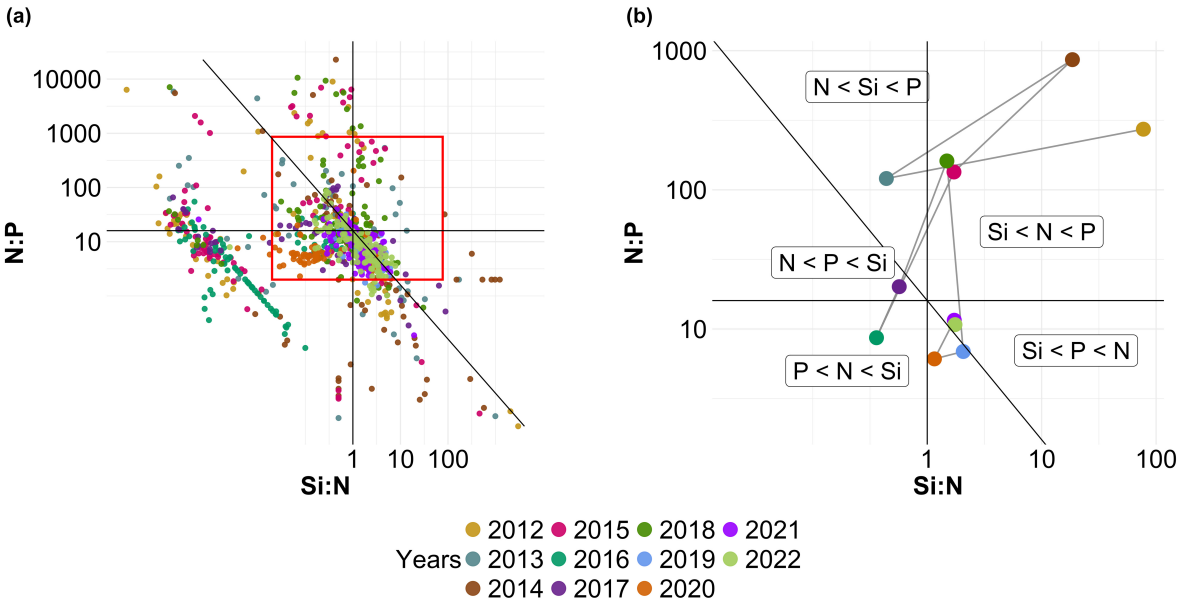

Figure 7. Evolution over time of potential N:P:Si nutrient limitations according to the ~~Redfield molar ratio~~ nutrient ratios (C:N:Si:P = 106:16:16:1; Redfield et al., 1963; Brzezinski, 1985). The horizontal black line represents the N:P limit of 16:1, the vertical black line the Si:N ratio of 1:1 and the diagonal black line the Si:P = 16:1 ratio. The red box (a) correspond to the zoom area (b). ~~The colors correspond to the average ratio for each year.~~ The (b) large colored dots correspond to the average ratio for each year ($N = 11$), while (a) the small lightened dots correspond to original of each year ($N = 1,015$). The expression A < B mean that B is potentially more limiting than A.

points identified previously with the cumulative sums of ~~nitrogen~~ $[NO_2^- + NO_3^-]$, phosphate and ~~silicate~~ Si (Fig. 6c, d, e). The analysis of these ratios across different seasons (see Appendix A1) reveals that, throughout our time series, winter has moved from a potential phosphate-limiting situation towards a slight nitrogen-limiting system. Additionally, the year 2014 exhibits indications of potential phosphate limitation across all seasons. Furthermore, autumn 2012 and, to a lesser extent, spring 2013 and summer 2018 demonstrate signs of potential phosphate limitation as well. ~~These seasonal variations are well reflected in the annual nutrient ratio~~ (Fig. 7).

3.3.2 Phytoplankton inter-annual dynamics

Environmental changes observed during the decadal survey have directly affected the biomass, abundance and composition of phytoplankton communities. The integrated analysis, combining total chlorophyll *a*, as a proxy of phytoplankton biomass and total abundance, revealed distinct patterns (Fig. 8). Chlorophyll *a* showed a succession of increasing and decreasing phases (Fig. 8a). The initial increase in biomass was notably influenced by the peak of 10.70 μg L^{-1} in February 2013. During the same year, phytoplankton abundance was remarkably low (Fig. 8b). After this phase, the chlorophyll *a* time series showed a decline, notably due to a weak spring bloom in 2016 towards higher values in 2018 and 2021. Despite these fluctuations, statistical tests on chlorophyll *a* concentration revealed no significant decadal trend (Table 4). Conversely, while total cell abundance showed

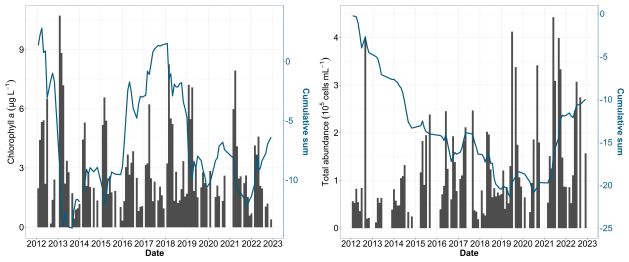

Figure 8. Time series of total phytoplankton biomass using (a) chlorophyll *a* and (b) total phytoplankton abundance. Bar plot represents monthly raw data for all stations combined (left y-axis). The blue lines represent the cumulative sum of anomalies over time (based on the difference between these monthly averages and the monthly average for the period, right y-axis).

interannual fluctuations with maximum values over $4 \cdot 10^6$ cell mL^{-1} in 2019 and 2021, analysis of raw data, cumulative sums and the Mann-Kendall test indicated a significant increase over the last decade (Fig. 8b and Table 4).

Over the past decade, notable changes in the structure of phytoplankton communities have been observed. Examination of raw data (Fig. 9, black bars) reveals pronounced seasonality, characterized by alternating periods of high and low abundance across all groups. This seasonality, broken down by group, is further presented in Fig. 5. Cumulative sums of various phytoplankton groups indicated a decadal increase in the abundance of OraPicoProk, RedPico, and OraNano over the period of our study (Fig. 9a, b, c). In 2021, OraPicoProk and RedPico exhibited their highest abundance. Furthermore, the high abundance recorded since 2019 for RedPico, significantly influenced the trends of these groups as well as the total phytoplankton abundance. Statistical trend analysis confirms a significant decadal increase in abundance of the latter two groups for all stations, as well as for total abundance (Table 4). OraNano depicted a clear trend for some nearshore and offshore stations as well, whereas a non-significant increase characterized frontal and offshore waters. The cumulative sum for RedNano depicts successive phases of increase until 2016, notably attributed to a robust bloom in 2015, followed by a decline until the series' conclusion (Fig. 9d). In spite of a more or less important decadal increase estimated in all stations, no significant trends were evidenced for RedNano. Conversely, RedMicro showed an overall decreasing trend, particularly evident since 2016, a significant trend was further confirmed at the most coastal stations (Fig. 9e, Table 4).

4 Discussion

~~Between 2012 and 2022, the DYPHYRAD time-series showed a significant decadal increase in temperature, changes in nutrient balance and an increase in phytoplankton abundance due to higher contribution of smaller cells. Spatial and temporal variability along the transect was highlighted throughout the decade, with a more or less pronounced spatial gradient from nearshore to offshore waters. We also identified for the first time a spatial and seasonal pattern of the environmental parameters, phytoplankton biomass and abundance of the six phytoplankton functional groups in the EEC.~~

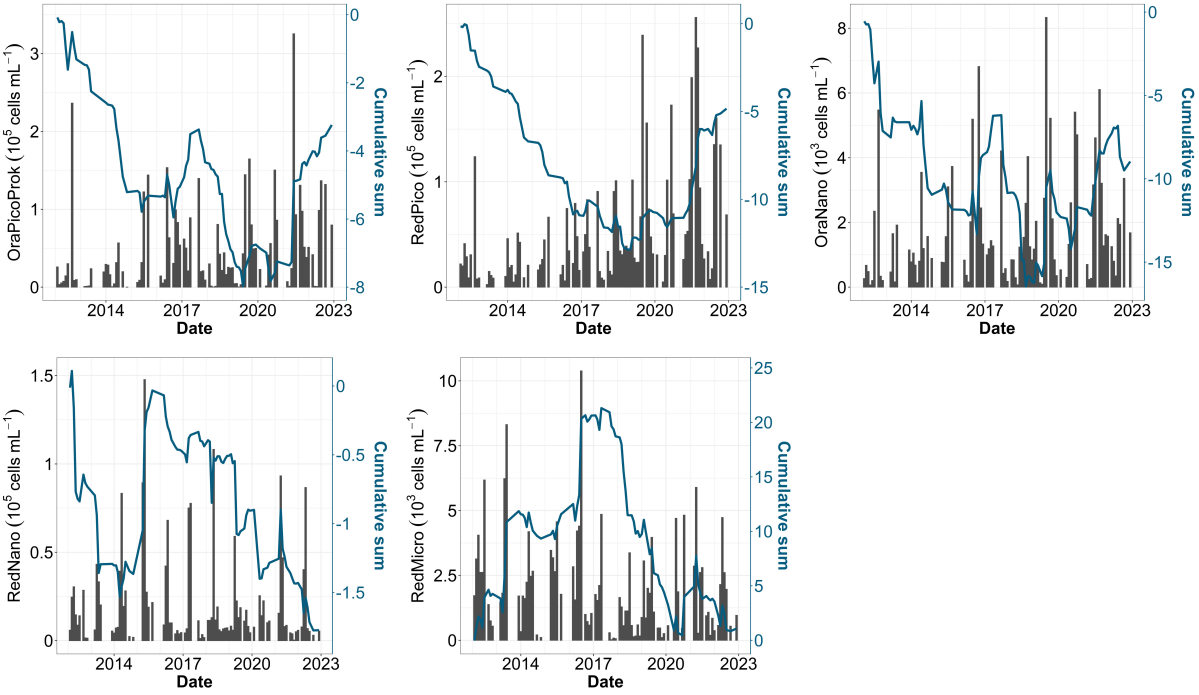

Figure 9. Time series of (a) total abundance, (b) OraPicoProk, (c) RedPico, (d) OraNano, (e) RedNano and (f) RedMicro. Bar plot represents monthly raw data for all stations combined (left y-axis). The blue lines represent the cumulative sum of anomalies over time (based on the difference between these monthly averages and the monthly average for the period, right y-axis).

Table 4. Trends and magnitude (slope) of change in phytoplankton chlorophyll *a*, total and functional groups abundance (cell mL^{-1}) determined by flow cytometry from Mann-Kendall test and Sen slope calculation. Bold indicates that the trend was significant (p-value < 0.05) over the period 2012-2022.

Phytoplankton biomass/abundance	R0	R0'	R1	R1'	R2	R2'	R3	R3'	R4
Chlorophyll *a* (μg L^{-1})	-0.034	-0.101	-0.096	+0.165	+0.248	-0.021	-0.104	-0.116	-0.386
Total abundance (cell mL^{-1})	**+8,214**	**+11,205**	**+8,542**	**+8,499**	**+9,983**	**+12,692**	**+15,446**	**+12,014**	**+9,278**
OraPicoProk (cell mL^{-1})	**+1,898**	**+2,550**	**+2,181**	+2,223	**+3,260**	**+3,921**	**+5,008**	**+4,075**	**+3,543**
RedPico (cell mL^{-1})	**+4,195**	**+6,345**	**+5,290**	**+5,372**	**+5,534**	**+7,731**	**+8,270**	**+7,901**	**+6,120**
OraNano (cell mL^{-1})	**+58**	+41	**+73**	+22	+22	+51	**+71**	**+66**	+68
RedNano (cell mL^{-1})	+5	+221	+ 32	+81	+50	+189	+311	+113	-161
RedMicro (cell mL^{-1})	**-122**	**-130**	-65	-106	-43	-71	-24	-50	-25

4.1 Decadal ~~Changes~~ trends in physical and chemical parameters

~~The observed decadal increase in sea surface temperature, considering monthly mean values along the transect,~~ Between 2012 and 2022, the DYPHYRAD time-series showed a significant decadal increase in SST range between +0.93 °C and +1.05 °C. This increase was in line with other studies carried out on a larger temporal and/or spatial scale in the English Channel with values between +0.3 °C per decade to over than +1 °C in 5 years (Saulquin and Gohin, 2010; McLean et al., 2019; Cornes et al., 2023). ~~While some longer-term investigations (spanning 30 years) failed to demonstrate this temperature rise (Lefebvre and Devreker, 2023 ; Tinker et al.,2020)~~ This general increase in SST is linked to an increase in the frequency of occurrence of maxima. Tinker et al. (2020) highlighted specific years, such as 2014, 2015 and 2017, as amongst the hottest ones on record for ~~sea surface temperature~~ SST over the past 125 years in the EEC region. Data for the year 2022 were not included in these earlier analyses, yet Simon et al. (2023) highlighted a pronounced marine heatwave in 2022, closely associated with exceptionally high air temperatures recorded during that summer (Guinaldo et al., 2023). This phenomenon was also recorded in our time series, which could further corroborate the trend towards increasing SST. This trend is likely to be consolidated in the coming years, as 2023 ranks as the second hottest year since 1991 (Météo-France). It is noteworthy that the influence of the Atlantic Multidecadal Oscillation (AMO), elucidated by Kerr (2000), has been acknowledged for ~~temperature~~ SST variations in the English Channel (Edwards et al., 2013; Auber et al., 2017). ~~However, despite these natural oscillations, the overall rise in water temperature may directly impact physico-chemical characteristics of water masses along the DYPHYRAD transect and affects its resident phytoplankton organisms (Richardson and Schoeman, 2004).~~ Regarding salinity, our study did not reveal any significant trends, even though the study of cumulative sums revealed a period of increasing salinity extending from winter 2014 to winter 2019, followed by a slight decrease during the last years. Salinity is a relatively stable physico-chemical parameter, however even the slightest change can have significant implications for the marine environment. Station BL1 (50°43'90 N; 1°33'00 E), located around 5.6 km south of our study area, has shown an increase in salinity since 1992 (Lefebvre and Devreker, 2023; Hernández-Fariñas et al., 2014). Increasing sea surface salinity can be attributed to the combined effects of rising sea surface ~~temperatures~~ SST and significant reduction in river flows between 1998 and 2019, particularly of the Seine and Somme rivers (Huguet et al., 2024). In our study of the Strait of Dover, the Somme, followed by the Canche, Authie, Liane, Wimereux and Slack, are the rivers that will influence the most our sampling area with increasingly low flow rates. The decrease in river flow over time may be due to a general decrease in rainfall distribution over the last decade (Météo-France). However, over the past decade, maximum values have tended to increase, which could lead to greater runoff and therefore higher concentrations of dissolved phosphate and silicate due to intense rainfall events. Indeed, silicate dynamics are linked to the weathering of rocks, 80 % of which are introduced into the ocean by rivers (Conley, 2002). Over the past decade, dissolved silicate indicated increasing silicate Si levels in frontal and offshore waters (from +1.08 to +1.39 μmol L^{-1}) and an increase in phosphate in nearshore waters (from +0.05 to +0.09 μmol L^{-1}) but decreased offshore (-0.026 μmol L^{-1}). A previous study at SRN station BL1 (off the port of Boulogne sur Mer) also showed a significant increase in dissolved silicate concentrations between 1992 and 2021 but decrease in phosphate (Lefebvre and Devreker, 2023). Long-term trend analysis showed a decrease in [NO_2^- + NO_3^-] (at least in nearshore waters) during the studied period. This decline confirmed substantiated by observations along

Boulogne-sur-Mer (transect BL), where [NO_2^- + NO_3^-] concentration exhibited a consistent decrease ranging from -0.63 to -1.72 μM over the two decade period (2000-2020 Lheureux et al., 2023). The dominant forms of dissolved nitrogen in the EEC are nitrite and nitrate, and are strongly influenced by continental inputs as well as Atlantic offshore inputs and atmospheric deposition (Dulière et al., 2019). The greater reduction in dissolved inorganic nitrogen in nearshore compared to offshore waters could be explained by a reduction in continental inputs due to lower river flows along the French coast (Huguet et al., 2024), combined with implementation of European directives (WFD and MSFD) aimed at reducing inputs of nitrogen and phosphorus into aquatic systems (Vigiak et al., 2023). Conversely, rising SST may lead to increased phosphate release from sediments, which could explain the rise in phosphate concentrations despite attenuation efforts (Wu et al., 2014; Vigiak et al., 2023). Added to these long-term trends are occasional events. The winter 2013-2014 emerged as a remarkable period during which [NO_2^- + NO_3^-] concentration was the highest. This is especially meaningful in the context of the extreme weather events of winter 2013-2014, characterized by strong storm events and unprecedented rainfall, resulting in remarkably high turbidity levels (Matthews et al., 2014; Gohin et al., 2015; Masselink et al., 2016). The high phosphate concentration was particularly notable in winter 2015 and 2019. These changes in temperature and nutrient concentration over the decade can modify stoichiometric ratio values (Redfield et al., 1963; Brzezinski, 1985) and led to different potential resources limitations in the environment and, therefore, affect composition and dynamics of phytoplankton communities.

4.2 ~~Change in nutrients concentrations and ratio~~ Consequences on phytoplankton functional groups

~~In the current study, the long-term trends in inorganic nutrients, essential for phytoplankton growth showed contrasting results. The trend analysis showed an increase in the monthly mean of nitrogen ([NO_2 + NO_3]) concentrations in the transect. On the other hand, the spatial trend analysis showed a decrease in nitrogen (at least in nearshore waters) during the studied period. This decline confirmed substantiated by observations along Boulogne-sur-Mer (transect BL), where nitrogen concentration exhibited a consistent decrease ranging from -0.63 to -1.72 μM over the two-decade period (2000-2020; Lheureux et al., 2023).~~ Rising temperatures SST, decreasing annual river flows, nitrogen depletion and modification in nutrient stoichiometry can lead to a decline in phytoplankton biomass, primary production and certain phytoplankton communities such as diatoms as shown in recent studies in the North Sea and English Channel (Capuzzo et al., 2018; Breton et al., 2022; Holland et al., 2023b). This phenomenon of microphytoplankton decreasing to the benefit of small cells, in particular *Synechococcus* spp. cyanobacteria, was described by Schmidt et al. (2020) in the Western English Channel (L4 station, 2007-2018). ~~The dominant forms of dissolved nitrogen in the EEC are nitrite and nitrate, and are strongly influenced by continental inputs as well as Atlantic offshore inputs and atmospheric deposition (Dulière et al., 2019) and showed significant seasonal variability. The greater reduction in dissolved inorganic nitrogen in nearshore compared to offshore waters could therefore be explained by a reduction in continental inputs. The winter 2013-2014 emerged as a remarkable period during which nitrogen concentration was the highest. This is especially meaningful in the context of the extreme weather events of winter 2013-2014, characterized by strong storm events and unprecedented rainfall, resulting in remarkably high turbidity levels (Matthews et al., 2014; Masselink et al.; Gohin et al., 2015).~~ Despite the natural oscillations, the overall rise in water SST may directly impact physico chemical characteristics of water masses along the DYPHYRAD transect and affects its resident phytoplankton organisms (Richardson

and Schoeman, 2004). Increasing temperature has a significant effect on the cell size of phytoplankton communities and shift to small species (Zohary et al., 2017; Sommer et al., 2017b; Zohary et al., 2021). Combined with a decrease in nutrient availability, this phenomenon is amplified from 4.7 % per °C to 46 % per °C (Peter and Sommer, 2013). El Hourany et al. (2021) showed the same behavior of phytoplankton communities (constant chlorophyll *a* concentration, decrease in diatoms abundance and increase in cyanobacteria abundance) in the Mediterranean when faced with a 0.4°C per decade increase in mean surface temperature. ~~Temporal trends on the cumulative sums revealed a steady decrease in silicate concentration, while spatial trends indicated increasing silicate levels in frontal and offshore waters. A previous study at the SRN station BL1 (off Boulogne-sur-Mer harbour) showed a significant increase in silicate concentrations between 1992 and 2021 ((Lefebvre and Devreker, 2023), which could be explained by the location and different sampling conditions. Silicate dynamics are linked to the weathering of rocks, 80 % of which are introduced into the ocean by rivers (Conley et al., 2002) and play a central role as the main limiting nutrient in the area (Lefebvre et al., 2011). Notably, diatoms, a key phytoplankton group, have shown a strong positive association with silicates availability and dissolved inorganic nitrogen (DIN; Leynaert et al., 2002; Hernández-Fariñas et al., 2014). During this study, our trend analysis showed an increase in phosphate (in nearshore waters) and a more complex pattern of variability in the cumulative sums with alternating increase and decrease phases. The high phosphate concentration was particularly notable in winter 2015 and 2019. According to Lefebvre et al. (2011), phosphate is the second most limiting nutrient after silica in the EEC. These changes in nutrient concentration over the decade can led to different potential resources limitations in the environment and, therefore, affect composition and dynamics of phytoplankton communities. Analysis of these annual limitations over time (Fig. 7) has shown that the ecosystem is not limited by nitrogen, unlike temperate coastal region where nitrogen generally limits primary production (Blomqvist et al., 2004). However, this limitation varies greatly with seasons and has a consequence for the succession of the phytoplankton communities. The imbalance associated with high nitrogen concentrations (although NH_4+ not measured in the present study) may be due to terrigenous inputs of nitrogen and phosphorus from intensive agriculture (Garnier et al., 2019). However, the decline in nitrogen levels in nearshore waters over the past decade can be attributed to the reduction in river flows along the French coast (Huguet et al., 2024) resulting in the application of European Directives (WFD and MSFD) that aimed at reducing nitrogen and phosphorus inputs into aquatic systems (Vigiak et al., 2023). Conversely, rising temperatures may lead to increased phosphate release from sediments, which could explain the rise in phosphate concentrations despite attenuation efforts (Wu et al., 2014, Vigiak et al., 2023).~~ Analysis of these annual limitations over time (Fig. 7) has shown that the ecosystem is not limited by nitrogen, unlike temperate coastal region where nitrogen generally limits primary production (Blomqvist et al., 2004). Indeed, Lefebvre et al. (2011) described dissolved silicate and phosphate as the most are the main limiting nutrient in the EEC. This limitation varies greatly with seasons and has a consequence for the succession of the phytoplankton communities. Notably, diatoms, a key phytoplankton group, have shown a strong positive association with dissolved silicate availability and dissolved inorganic nitrogen (DIN; Leynaert et al., 2002; Hernández-Fariñas et al., 2014). Over the past decade, we observed similar trends in nutrient ratios as observed for the SOMLIT coastal station, with a decrease in N:P, Si:P and Si:N ratios. ~~In addition,~~ Lheureux et al. (2023) documented an increase in Si:P and Si:N ratios at the SRN station in Boulogne-sur-Mer, while the SOMLIT (National Observation Service of the Research Infrastructure ILICO) coastal station (South of Boulogne-sur-Mer and further offshore) showed a decrease in all

N:P, Si:P and Si:N ratios as in our study. Under low nutrient conditions, small cells are indeed more competitive under low nutrient conditions (Sommer et al., 2017a) because of lower resource requirement and higher Surface:Volume ratio. However, they are less nutritious primary producers of higher food webs organisms, which can lead to a decline in higher trophic levels (Schmidt et al., 2020; Holland et al., 2023b). Sommer et al. (2017b) also predict that with a smaller phytoplankton community, a greater proportion of primary production will benefit the microbial food web, to the detriment of the classic grazing food chain. ~~In our study, we observed similar trends in nutrient ratios as observed for the SOMLIT coastal station, with a decrease in ratios over the last decade.~~

4.3 ~~Changes in phytoplankton biomass and abundance~~

~~Rising temperatures, decreasing annual river flows, nitrogen depletion and nutrient imbalances can lead to a decline in phytoplankton biomass, primary production and certain phytoplankton communities such as diatoms as shown in recent studies in the North Sea and English Channel (Holland et al., 2023, Breton et al., 2022, Capuzzo et al., 2018). A decline in chlorophyll a (as a proxy of phytoplankton biomass) has already been described in the EEC using satellite images for the last two decades (Hughuet et al., 2024, Gohin et al., 2019). No significant trend in chlorophyll a could be identified in the present work, however the cumulative sums did reveal successive phases after an initial decrease in chlorophyll a until 2013, followed by an increase until 2018 and then a decrease until 2022. The year 2013, in addition to being the coldest in the series, also presented a potential limitation in phosphate and silicate, which can be detrimental to the growth of large phytoplankton groups (e.g. most diatoms). The year 2018 is also a year of silicate and nitrogen limitation. These years both followed years of lower riverine input to the Somme (2012 and 2017; HydroPortail, https://www.hydro.eaufrance.fr/), which may have influenced nutrient inputs in subsequent years. In contrasting ways, high nitrogen concentration (including NH_4^+), phosphorus limitation or environmental nutrient imbalances favor haptophyte species such as Phaeocystis globosa, able to take advantage of remaining resources (Tungaraza et al., 2003, Lancelot et al. 2011, Lefebvre et al. 2011, Breton et al., 2022. These results align with seasonal observations, including the phosphate-limited spring of 2015 and the RedNano bloom peak recorded in our study. In the Southern North Sea and the EEC, RedNano is known to be largely dominated by Phaeocystis globosa during spring blooms (Guiselin, 2010, Thyssen et al., 2015, Bonato et al., 2015, Louchart et al., 2024). The decline in nearshore nitrogen levels and the return to nearly equilibrium values of the N:Si:P (16:16:1) ratio since 2016 could potentially reduce Phaeocystis globosa blooms, to the benefit of other species or functional groups, consistent with trends observed in RedNano cumulative sums. The positive correlation between nitrogen availability, particularly during winter, and chlorophyll a concentration has been corroborated (Lefebvre and Dezécache, 2020). Dissolved Inorganic Nitrogen (DIN) decrease during the time-series (1994-2018) was associated with an increase in diatoms (notably Pseudo-nitzchiza) and a decrease in Phaeocystis globosa in the high DIN concentration area (Lefebvre and Dezécache, 2020). If such a trend in nitrite and nitrate concentrations persists, spring blooms of Phaeocystis globosa could be reduced. The use of flow cytometry for long-term in vivo monitoring of phytoplankton communities has revealed a change in size structure. The EEC experienced a significant increase in the total abundance of cells mainly because of picoeukaryotes and Synechococcus spp.. As absolute and relative abundance of picophytoplankton increased, nano– (to some extent) and microphytoplankton decreased. This phenomenon of microphytoplankton decreasing to~~

~~the benefit of small cells, in particular Synechococcus spp. cyanobacteria, was described by Schmidt et al. (2020) in the Western English Channel (L4 station, 2007–2018). These cells are indeed more competitive under low nutrient conditions (Sommer et al, 2017a) because of lower resource requirement and higher Surface:Volume ratio. However, they are less nutritious primary producers of higher food webs organisms, which can lead to a decline in higher trophic levels (Schmidt et al., 2020, Holland et al., 2023).~~

4.4 Phytoplankton variability dominated by seasonality

Our study showed that seasons explained more than 50 % of the variability observed in phytoplankton communities. This seasonality has been described in numerous studies, notably in regards to the spring bloom of *Phaeocystis globosa*, which can account for up to 80 % of the total phytoplankton biomass in the EEC (Bonato et al., 2016; Guiselin, 2010). The rest of the time, phytoplankton biomass determined by microscope observation (thus excluding picophytoplankton and small nanophytoplankton) is mainly dominated by diatoms and can reach 85 % of total phytoplankton biomass (Breton et al., 2000; Lefebvre et al., 2011; Hernández-Fariñas et al., 2014). In terms of abundance, cyanobacteria, ~~picoeucaryotes~~ picoeukaryotes and *Phaeocystis globosa* dominate the area (Bonato et al., 2016). Winter and summer periods are dominated, in terms of abundance, by *Synechococcus* spp. and ~~picoeucaryotes~~ picoeukaryotes (Bonato et al., 2016), although they may not share the same niches/habitats (Louchart et al., 2024) which allow them to bloom at the same period (Fig. 5). Other groups are also present in lower abundances, such as cryptophytes, coccolithophores and dinoflagellates (Hernández-Fariñas et al., 2014; Bonato et al., 2016). The spatial gradient is present for most groups and strongly marked for nano- and microphytoplankton, with abundances sometimes three times higher at the coast especially during bloom periods because there are more resources available nearshore (due to the inputs from the rivers). During the autumn-winter period, changes in spatial community structure was observed with lower abundance of dominant chlorophyll *a* nanophytoplankton at nearshore (R0) and offshore (R4) stations than at frontal stations (R1'and R2). This spatial conformation can be explained by the action of coastal flow on water bodies, as well as by the action of tides and wind speed and direction (Brylinski et al., 1991; Sentchev and Yaremchuk, 2007). This accumulation of nanophytoplankton in the frontal zones has already been shown in the southern North Sea to be linked to the greater presence of nutrients in these structures than in other bodies of water (Gieskes et al., 2007). Our study has also highlighted the importance of bottom-up control in phytoplankton abundance and biomass distribution, but other parameters such as zooplankton predation (Cotonnec et al., 2001; Breton et al., 2021) and seasonal bacterial/microbial and viral interactions can play a significant role in phytoplankton community variability (Brussaard, 2004; Lamy et al., 2009).

4.5 General discussion, limitations and perspectives

The sampling strategy within DYPHYRAD surveys allowed acquiring additional data at higher sampling frequencies and finer spatial scales than other monitoring networks of phytoplankton-related variables (SOMLIT, SRN-REPHY, PHYTOBS). If our approach is also characterized by a fine spatial resolution, its temporal resolution is lower than high frequency moorings or automated stations of French national Coast-HF network (as the MAREL-Carnot automated station off Boulogne-sur-Mer; Halawi Ghosn et al., 2023). Moreover, our surveys made it possible to decouple stations in order to account for the entire

coastal-offshore gradient – a frontal zone separating waters influenced by desalination from river inputs and offshore waters under a macrotidal regime, accounting for tidal variability. Most long-term studies on the evolution of phytoplankton communities over time are either based on the evolution of chlorophyll *a* as a proxy for phytoplankton biomass to explain changes linked to environmental parameters, or based on taxonomical phytoplankton counts by microscopy. However, this kind of approach does not seem sufficient, as it neglects the influence of smaller groups (e.g. picoeukaryotes, cyanobacteria, small nanophytoplankton; McQuatters-Gollop et al., 2024) which play an essential role in food webs. The advantage of automated pulse-shape flow cytometry is that the methodology is the same for analysis of the entire phytoplankton size range (Dubelaar et al., 2004), *in vivo*, avoiding any damage or effect of fixatives. The optical characteristics of each particle can then be used to monitor not only abundance, but also functional traits specific to each phytoplankton functional group (Fontana et al., 2018; Fragoso et al., 2019; Louchart et al., 2020). Although this method enables us to study all phytoplankton, it is not a taxonomic technique (except in the case of microphytoplankton via CytoSense photo acquisition) and could be combined with approaches enabling finer identification. In order to exploit these features and upscale such results over the long term, it remains essential to improve standard operating procedures for better intercomparability and interoperability between machines, work still in progress in the frame of current international projects as JERICO S3 and OBAMA NEXT.

5 Conclusions

This local-scale study showed an increase in ~~sea surface temperature~~ SST, nearshore phosphate and offshore ~~silicate~~ dissolvedSi, as well as a decrease in ~~nitrogen (nitrite and nitrate)~~ $[NO_2^- + NO_3^-]$ concentration in nearshore water over the last decade. Pulse-shape flow cytometry time series allowed to explore the spatio-temporal *in vivo* dynamics of almost the whole phytoplankton community. A significant increase in small phytoplankton (including cyanobacteria) and a decrease in microphytoplankton abundance (in coastal water) were evidenced. While our time series is too short to draw definitive conclusions about long-term and complex climate change impacts, it allows us to make an initial assessment of change within phytoplankton communities in the EEC by the Strait of Dover. Recent studies increasingly indicate that climate change is a driver of major alterations in oceanic and coastal ecosystems particularly through the increase of sea surface temperature and nutrient availability (Pörtner et al., 2022). Such environmental transformation influence phytoplankton community size with the favor of smaller phytoplankton species and cyanobactereia, wich are more adaptable to warmer and nutrient-variable conditions (Sommer et al., 2017b; Zohary et al., 2017, 2021). The reduction in microphytoplancton observed here could signify a broader shift toward smaller phytoplankton sizes in response to these pressures, impacting trophic dynamics by influencing size-grazing, nutrient consumption, sedimentation and limiting energy transfer efficiency within the food web. As climate models predict continued warming and nutrient shifts (Pörtner et al., 2022), these initial changes observed in the Strait of Dover may signal a broader trend, making sustained monitoring and high resolution data critical to anticipate long-term impacts on marine biodiversity and ecosystem stability. It is crucial to sustain sampling efforts using automated techniques like flow cytometry to monitor exhaustively the evolution of phytoplankton dynamics. This monitoring should be integrated as a complement of existing low-frequency reference national and regional observation networks, and incorporated into high-frequency surveyx as carried out in

short-term previous studies on automated stations (Thyssen et al., 2014; Robache, in prep), ships of opportunity (Marrec et al., 2021) and oceanographic cruises (Bonato et al., 2016; Louchart et al., 2020, 2024). Supported by a more comprehensive characterization of PFGs, this approach will greatly enhance our understanding of the impacts of global and anthropogenic changes on phytoplankton functional diversity. Moreover, when coupled with productivity measurements (Aardema et al., 2019) and integrated into predictive models, it becomes possible to evaluate the potentialities of food web evolution and overall ecosystem functioning.

Appendix A: Seasonal nutrients limitation

To study the evolution of nutrient limitation in more detail within the annual evolution, we analyzed seasonal N:P:Si ratios (Nitrogen/Phosphate/~~Silicate~~ Dissolved silicate; Fig. A1). This representation shows a near-constancy in winters with little or no potential ~~silicate~~ Si limitation and slight phosphate or nitrogen limitation. Spring shows a potential phosphate limitation for the years 2013, 2014, 2015 and 2018, while the other years do not seem to be limited or slightly limited by ~~silicate~~ Si or nitrogen. Autumn 2015 and 2020 appear to be potentially ~~silicate~~ Si-limiting, whereas 2012 and 2014 show a clear phosphate limitation. Summer 2014 and 2018 tend to be slightly potentially phosphate-limiting, while summer 2013, 2015 and 2016 tend to be potentially ~~silicate~~ Si-limiting. The other summers do not appear to be limiting or at least slightly potentially nitrogen limiting, according to the data presented here.

Appendix B: Tukey post-hoc test results

Data availability. A data paper (Hubert, in prep) is in preparation. Data will be made available on request.

Author contributions. ZH, LFA and SM conceived and designed the study. ZH performed the data treatment, the code and the analysis of data under the supervision of SM and LFA and advise of AE, KR (figure optimization) and AL (GAM analysis). CG, VC, MC and EL contributed to data collection and production. ZH wrote the first manuscript draft and all authors contribued to the final version.

Competing interests. The authors declare that they have no known competing financial interests or personal relationships that could have appeared to influence the work reported in this paper.

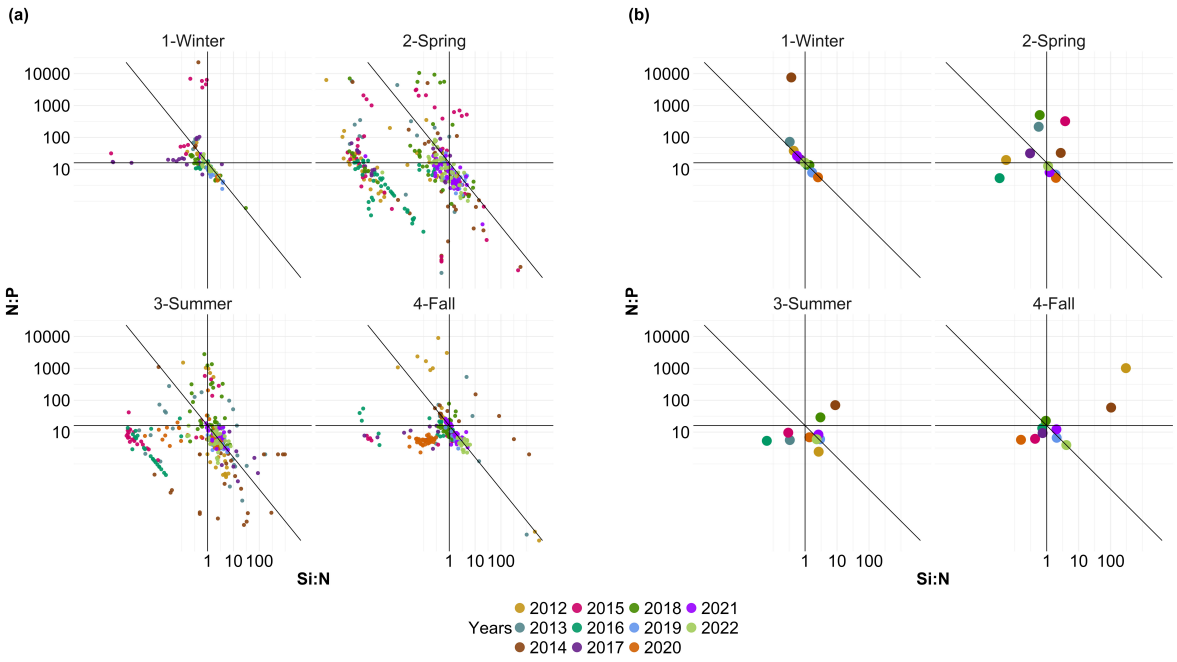

Figure A1. Evolution over seasons of potential N:P:Si nutrient limitations according to the ~~Redfield molar ratio~~ nutrient ratios (C:N:Si:P = 106:16:16:1; Redfield et al., 1963; Brzezinski, 1985). The horizontal line represents the N:P limit of 16:1, the vertical line the Si:N ratio of 1:1 and the diagonal line the Si:P = 16:1 ratio. ~~The colors correspond to the average ratio for each year.~~ (a) Small dots correspond to original of each year ($N = 1{,}015$). (b) The colored dots correspond to the average ratio for each year and season ($N = 44$).

Acknowledgements. We would like to thank the crew (Christophe Routtier and Noël Lefilliatre) of the research vessel *Sepia II* (CNRS INSU, French National Oceanographic Fleet) as well as Eric Lécuyer for CTD data and also students and interns of LOG which helped in the collection and production of environmental data since 2012. We are also grateful to Eric Lécuyer for his constructive remarks to improve the discussion. ZH is supported by a Doctorate grant from the Région Hauts-de-France and Université du Littoral Côte d'Opale (ULCO) and the Doctoral School ED STS (UPJV, UA, ULCO). DYPHYRAD (P.I. LFA) monitoring of phytoplankton was initiated with the support of the INTERREG IV A "2 Seas" DYMAPHY project (2010-2014, P.I. LFA), followed by the JERICO NEXT (2015-2019) and S3 (2020-2024) H2020 European projects. Monitoring was also supported by French State and Nord-Pas-de-Calais–Hauts-de-France Regional Contracts (CPER) *Phaeocystis* Bloom (2001-2008) and MARCO (2015-2021), which supported the purchase of CytoSense and CytoSub sensors and by CPER IDEAL and its Observation, Geomatic and Remote Sensing technical platform (2021-2028). This work is also supported by the Priority Research Project "Ocean and Climate" PPR RioMAR supported by a France 2030 grant (ANR-22-POE-0006) and the Graduate School IFSEA that also benefits from a France 2030 grant (ANR-21-EXES-0011) operated by the French National Research Agency. Part of this work was supported by the JERICO-S3 project, receiving funding from the European Union's Horizon 2020 research and innovation programme under grant agreement n° 871153 and by the OBAMA NEXT project under European Union's grant agreement 101081642. We would like to thank the French national observation network SOMLIT and the ILICO research infrastructure. We are grateful to the two anonymous reviewers who contributed to improve this article.

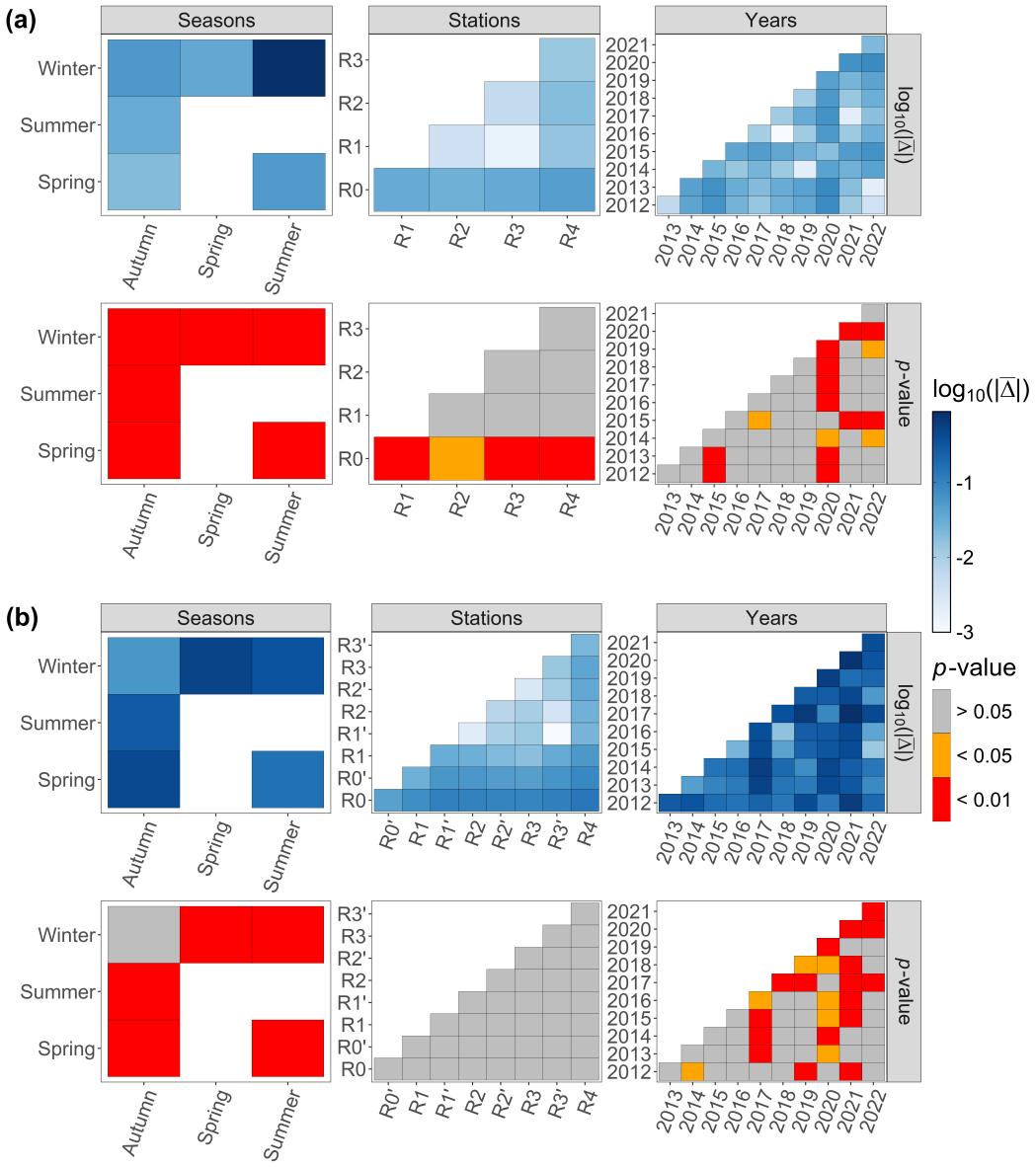

Figure B1. Tukey post-hoc results for (a) environmental data and (b) phytoplankton abundance data. The absolute value of the mean difference provided by the test (noted $|\overline{\Delta}|$) and the associated p-value are provided.

References

Aardema, H. M., Rijkeboer, M., Lefebvre, A., Veen, A., and Kromkamp, J. C.: High-Resolution Underway Measurements of Phytoplankton Photosynthesis and Abundance as an Innovative Addition to Water Quality Monitoring Programs, Ocean Science, 15, 1267–1285, https://doi.org/10.5194/os-15-1267-2019, 2019.

Akanmu, R.: Nutrients Dynamics and Trophic Status in A Tropical Ocean off The Lagos Coast, Nigeria, pp. 87–99, 2018.

Aminot, A. and Kérouel, R.: Dosage automatique des nutriments dans les eaux marines: méthodes en flux continu, Editions Quae, ISBN 978-2-7592-0023-8, 2007.

Auber, A., Gohin, F., Goascoz, N., and Schlaich, I.: Decline of Cold-Water Fish Species in the Bay of Somme (English Channel, France) in Response to Ocean Warming, Estuarine, Coastal and Shelf Science, 189, 189–202, https://doi.org/10.1016/j.ecss.2017.03.010, 2017.

Barton, A. D., Pershing, A. J., Litchman, E., Record, N. R., Edwards, K. F., Finkel, Z. V., Kiørboe, T., and Ward, B. A.: The Biogeography of Marine Plankton Traits, Ecology Letters, 16, 522–534, https://doi.org/10.1111/ele.12063, 2013.

Blomqvist, S., Gunnars, A., and Elmgren, R.: Why the Limiting Nutrient Differs between Temperate Coastal Seas and Freshwater Lakes: A Matter of Salt, Limnology and Oceanography, 49, 2236–2241, https://doi.org/10.4319/lo.2004.49.6.2236, 2004.

Bonato, S., Christaki, U., Lefebvre, A., Lizon, F., Thyssen, M., and Artigas, L. F.: High Spatial Variability of Phytoplankton Assessed by Flow Cytometry, in a Dynamic Productive Coastal Area, in Spring: The Eastern English Channel, Estuarine, Coastal and Shelf Science, 154, 214–223, https://doi.org/10.1016/j.ecss.2014.12.037, 2015.

Bonato, S., Breton, E., Didry, M., Lizon, F., Cornille, V., Lécuyer, E., Christaki, U., and Artigas, L. F.: Spatio-Temporal Patterns in Phytoplankton Assemblages in Inshore–Offshore Gradients Using Flow Cytometry: A Case Study in the Eastern English Channel, Journal of Marine Systems, 156, 76–85, https://doi.org/10.1016/j.jmarsys.2015.11.009, 2016.

Breton, E., Brunet, C., Sautour, B., and Brylinski, J.-M.: Annual Variations of Phytoplankton Biomass in the Eastern English Channel: Comparison by Pigment Signatures and Microscopic Counts, Journal of Plankton Research, 22, 1423–1440, https://doi.org/10.1093/plankt/22.8.1423, 2000.

Breton, E., Christaki, U., Bonato, S., Didry, M., and Artigas, L. F.: Functional Trait Variation and Nitrogen Use Efficiency in Temperate Coastal Phytoplankton, Marine Ecology Progress Series, 563, 35–49, https://doi.org/10.3354/meps11974, 2017.

Breton, E., Christaki, U., Sautour, B., Demonio, O., Skouroliakou, D.-I., Beaugrand, G., Seuront, L., Kléparski, L., Poquet, A., Nowaczyk, A., Crouvoisier, M., Ferreira, S., Pecqueur, D., Salmeron, C., Brylinski, J.-M., Lheureux, A., and Goberville, E.: Seasonal Variations in the Biodiversity, Ecological Strategy, and Specialization of Diatoms and Copepods in a Coastal System With *Phaeocystis Blooms*: The Key Role of Trait Trade-Offs, Frontiers in Marine Science, 8, 2021.

Breton, E., Goberville, E., Sautour, B., Ouadi, A., Skouroliakou, D.-I., Seuront, L., Beaugrand, G., Kléparski, L., Crouvoisier, M., Pecqueur, D., Salmeron, C., Cauvin, A., Poquet, A., Garcia, N., Gohin, F., and Christaki, U.: Multiple Phytoplankton Community Responses to Environmental Change in a Temperate Coastal System: A Trait-Based Approach, Frontiers in Marine Science, 9, 2022.

Breton, E., Savoye, N., Rimmelin-Maury, P., Sautour, B., Goberville, E., Lheureux, A., Cariou, T., Ferreira, S., Agogué, H., Alliouane, S., Aubert, F., Aubin, S., Berthebaud, E., Blayac, H., Blondel, L., Boulart, C., Bozec, Y., Bureau, S., Caillo, A., Cauvin, A., Cazes, J.-B., Chasselin, L., Claquin, P., Conan, P., Cordier, M.-A., Costes, L., Crec'hriou, R., Crispi, O., Crouvoisier, M., David, V., Del Amo, Y., De Lary, H., Delebecq, G., Devesa, J., Domeau, A., Durozier, M., Emery, C., Feunteun, E., Fauchot, J., Gentilhomme, V., Geslin, S., Giraud, M., Grangeré, K., Grégori, G., Grossteffan, E., Gueux, A., Guillaudeau, J., Guillou, G., Harrewyn, M., Jolly, O., Jude-Lemeilleur, F., Labatut, P., Labourdette, N., Lachaussée, N., Lafont, M., Lagadec, V., Lambert, C., Lamoureux, J., Lanceleur, L., Lebreton, B., Lecuyer,

E., Lemeille, D., Leredde, Y., Leroux, C., Leynaert, A., L'Helguen, S., Liénart, C., Macé, E., Maria, E., Marie, B., Marie, D., Mas, S., Mendes, F., Mornet, L., Mostajir, B., Mousseau, L., Nowaczyk, A., Nunige, S., Parra, R., Paulin, T., Pecqueur, D., Petit, F., Pineau, P., Raimbault, P., Rigaut-Jalabert, F., Salmeron, C., Salter, I., Sauriau, P.-G., Seuront, L., Sultan, E., Valdès, R., Vantrepotte, V., Vidussi, F., Voron, F., Vuillemin, R., Zudaire, Laurent., and Garcia, N.: Data Quality Control Considerations in Multivariate Environmental Monitoring: Experience of the French Coastal Network SOMLIT, Frontiers in Marine Science, 10, https://doi.org/10.3389/fmars.2023.1135446, 2023.

Brussaard, C. P. D.: Viral Control of Phytoplankton Populations—a Review[1], Journal of Eukaryotic Microbiology, 51, 125–138, https://doi.org/10.1111/j.1550-7408.2004.tb00537.x, 2004.

Brylinski, J. M., Lagadeuc, Y., Gentilhomme, V., Dupont, J. P., Lafite, R., Dupeuble, P. A., Huault, M. F., and Auger, Y.: Le "fleuve côtier" : Un phénomène hydrologique important en Manche orientale. Exemple du Pas-de-Calais, Oceanologica Acta, Special issue, 1991.

Brzezinski, M. A.: The Si:C:N Ratio Of Marine Diatoms: Interspecific Variability And The Effect Of Some Environmental Variables, Journal of Phycology, 21, 347–357, https://doi.org/10.1111/j.0022-3646.1985.00347.x, 1985.

Capuzzo, E., Lynam, C. P., Barry, J., Stephens, D., Forster, R. M., Greenwood, N., McQuatters-Gollop, A., Silva, T., van Leeuwen, S. M., and Engelhard, G. H.: A Decline in Primary Production in the North Sea over 25 Years, Associated with Reductions in Zooplankton Abundance and Fish Stock Recruitment, Global Change Biology, 24, e352–e364, https://doi.org/10.1111/gcb.13916, 2018.

Cloern, J. E., Abreu, P. C., Carstensen, J., Chauvaud, L., Elmgren, R., Grall, J., Greening, H., Johansson, J. O. R., Kahru, M., Sherwood, E. T., Xu, J., and Yin, K.: Human Activities and Climate Variability Drive Fast-Paced Change across the World's Estuarine–Coastal Ecosystems, Global Change Biology, 22, 513–529, https://doi.org/10.1111/gcb.13059, 2016.

Conley, D. J.: Terrestrial Ecosystems and the Global Biogeochemical Silica Cycle, Global Biogeochemical Cycles, 16, 68–1–68–8, https://doi.org/10.1029/2002GB001894, 2002.

Cooley, S., Schoeman, D., Bopp, L., Boyd, P., Donner, S., Ito, S.-i., Kiessling, W., Martinetto, P., Ojea, E., Racault, M.-F., Rost, B., Skern-Mauritzen, M., Ghebrehiwet, D. Y., Bell, J. D., Blanchard, J., Bolin, J., Cheung, W. W. L., Cisneros-Montemayor, A., Dupont, S., Dutkiewicz, S., Frölicher, T., Gaitán-Espitia, J.-D., Molinos, J. G., Gurney-Smith, H., Henson, S., Hidalgo, M., Holland, E., Kopp, R., Kordas, R., Kwiatkowski, L., Le Bris, N., Lluch-Cota, S. E., Logan, C., Mark, F. C., Mgaya, Y., Moloney, C., Muñoz Sevilla, N. P., Randin, G., Raja, N. B., Rajkaran, A., Richardson, A., Roe, S., Ruiz Diaz, R., Salili, D., Sallée, J.-B., Scales, K., Scobie, M., Simmons, C. T., Torres, O., and Yool, A.: Chapter 3: Oceans and Coastal Ecosystems and Their Services, https://www.ipcc.ch/report/ar6/wg2/downloads/report/IPCC_AR6_WGII_FinalDraft_Chapter03.pdf, 2022.

Cornes, R. C., Tinker, J., Hermanson, L., Oltmanns, M., Hunter, W. R., Lloyd-Hartley, H., Kent, E. C., Rabe, B., and Renshaw, R.: The Impacts of Climate Change on Sea Temperature around the UK and Ireland, https://nora.nerc.ac.uk/id/eprint/534103/, 2023.

Cotonnec, G., Brunet, C., Sautour, B., and Thoumelin, G.: Nutritive Value and Selection of Food Particles by Copepods During a Spring Bloom of *Phaeocystis Sp.* in the English Channel, as Determined by Pigment and Fatty Acid Analyses, Journal of Plankton Research, 23, 693–703, https://doi.org/10.1093/plankt/23.7.693, 2001.

Dubelaar, G. B. J., Geerders, P. J. F., and Jonker, R. R.: High Frequency Monitoring Reveals Phytoplankton Dynamics, Journal of Environmental Monitoring, 6, 946–952, https://doi.org/10.1039/B409350J, 2004.

Dulière, V., Gypens, N., Lancelot, C., Luyten, P., and Lacroix, G.: Origin of Nitrogen in the English Channel and Southern Bight of the North Sea Ecosystems, Hydrobiologia, 845, 13–33, https://doi.org/10.1007/s10750-017-3419-5, 2019.

Edwards, M., Beaugrand, G., Helaouët, P., Alheit, J., and Coombs, S.: Marine Ecosystem Response to the Atlantic Multidecadal Oscillation, PLOS ONE, 8, e57 212, https://doi.org/10.1371/journal.pone.0057212, 2013.

El Hourany, R., Mejia, C., Faour, G., Crépon, M., and Thiria, S.: Evidencing the Impact of Climate Change on the Phytoplankton Community of the Mediterranean Sea Through a Bioregionalization Approach, Journal of Geophysical Research: Oceans, 126, e2020JC016 808, https://doi.org/10.1029/2020JC016808, 2021.

Falkowski, P., Scholes, R. J., Boyle, E., Canadell, J., Canfield, D., Elser, J., Gruber, N., Hibbard, K., Högberg, P., Linder, S., Mackenzie, F. T., Moore III, B., Pedersen, T., Rosenthal, Y., Seitzinger, S., Smetacek, V., and Steffen, W.: The Global Carbon Cycle: A Test of Our Knowledge of Earth as a System, Science, 290, 291–296, https://doi.org/10.1126/science.290.5490.291, 2000.

Falkowski, P. G. and Oliver, M. J.: Mix and Match: How Climate Selects Phytoplankton, Nature Reviews Microbiology, 5, 813–819, https://doi.org/10.1038/nrmicro1751, 2007.

Fontana, S., Thomas, M. K., Moldoveanu, M., Spaak, P., and Pomati, F.: Individual-Level Trait Diversity Predicts Phytoplankton Community Properties Better than Species Richness or Evenness, The ISME Journal, 12, 356–366, https://doi.org/10.1038/ismej.2017.160, 2018.

Fragoso, G. M., Poulton, A. J., Pratt, N. J., Johnsen, G., and Purdie, D. A.: Trait-Based Analysis of Subpolar North Atlantic Phytoplankton and Plastidic Ciliate Communities Using Automated Flow Cytometer, Limnology and Oceanography, 64, 1763–1778, https://doi.org/10.1002/lno.11189, 2019.

Garcia, N. and Oriol, L.: Analyse Automatique Des Nutriments NO_2 - NO_3 - PO_4 - $Si(OH)_4$ Dans l'eau de Mer. Procédure : Protocole National Sels Nutritifs, Tech. rep., SOMLIT, 2019.

Gieskes, W. W. C., Leterme, S. C., Peletier, H., Edwards, M., and Reid, P. C.: *Phaeocystis* Colony Distribution in the North Atlantic Ocean since 1948, and Interpretation of Long-Term Changes in the *Phaeocystis* Hotspot in the North Sea, Biogeochemistry, 83, 49–60, https://doi.org/10.1007/s10533-007-9082-6, 2007.

Gohin, F., Bryère, P., and Griffiths, J. W.: The Exceptional Surface Turbidity of the North-West European Shelf Seas during the Stormy 2013–2014 Winter: Consequences for the Initiation of the Phytoplankton Blooms?, Journal of Marine Systems, 148, 70–85, https://doi.org/10.1016/j.jmarsys.2015.02.001, 2015.

Gohin, F., Van der Zande, D., Tilstone, G., Eleveld, M. A., Lefebvre, A., Andrieux-Loyer, F., Blauw, A. N., Bryère, P., Devreker, D., Garnesson, P., Hernández Fariñas, T., Lamaury, Y., Lampert, L., Lavigne, H., Menet-Nedelec, F., Pardo, S., and Saulquin, B.: Twenty Years of Satellite and *in Situ* Observations of Surface Chlorophyll-*a* from the Northern Bay of Biscay to the Eastern English Channel. Is the Water Quality Improving?, Remote Sensing of Environment, 233, 111 343, https://doi.org/10.1016/j.rse.2019.111343, 2019.

Guinaldo, T., Voldoire, A., Waldman, R., Saux Picart, S., and Roquet, H.: Response of the Sea Surface Temperature to Heatwaves during the France 2022 Meteorological Summer, Ocean Science, 19, 629–647, https://doi.org/10.5194/os-19-629-2023, 2023.

Guiselin, N.: Etude de La Dynamique Des Communautés Phytoplanctoniques Par Microscopie et Cytométrie En Flux, En Eaux Côtière de La Manche Orientale, Ph.D. thesis, Université du Littoral Côté d'Opale, France, 2010.

Halawi Ghosn, R., Poisson-Caillault, É., Charria, G., Bonnat, A., Repecaud, M., Facq, J.-V., Quéméner, L., Duquesne, V., Blondel, C., and Lefebvre, A.: MAREL Carnot Data and Metadata from the Coriolis Data Center, Earth System Science Data, 15, 4205–4218, https://doi.org/10.5194/essd-15-4205-2023, 2023.

Henson, S. A., Cole, H. S., Hopkins, J., Martin, A. P., and Yool, A.: Detection of Climate Change-Driven Trends in Phytoplankton Phenology, Global Change Biology, 24, e101–e111, https://doi.org/10.1111/gcb.13886, 2018.

Hernández-Fariñas, T., Soudant, D., Barillé, L., Belin, C., Lefebvre, A., and Bacher, C.: Temporal Changes in the Phytoplankton Community along the French Coast of the Eastern English Channel and the Southern Bight of the North Sea, ICES Journal of Marine Science, 71, 821–833, https://doi.org/10.1093/icesjms/fst192, 2014.

Hillebrand, H., Acevedo-Trejos, E., Moorthi, S. D., Ryabov, A., Striebel, M., Thomas, P. K., and Schneider, M.-L.: Cell Size as Driver and Sentinel of Phytoplankton Community Structure and Functioning, Functional Ecology, 36, 276–293, https://doi.org/10.1111/1365-2435.13986, 2022.

Holland, M., Louchart, A., Artigas, L. F., and Mcquatters-Gollop, A.: Changes in Phytoplankton and Zooplankton Communities Common Indicator Assessment Changes in Phytoplankton and Zooplankton Communities, in: OSPAR, 2023: The 2023 Quality Status Report for the Northeast Atlantic., p. 39, OSPAR Commission, 2023a.

Holland, M. M., Louchart, A., Artigas, L. F., Ostle, C., Atkinson, A., Rombouts, I., Graves, C. A., Devlin, M., Heyden, B., Machairopoulou, M., Bresnan, E., Schilder, J., Jakobsen, H. H., Lloyd-Hartley, H., Tett, P., Best, M., Goberville, E., and McQuatters-Gollop, A.: Major Declines in NE Atlantic Plankton Contrast with More Stable Populations in the Rapidly Warming North Sea, Science of The Total Environment, 898, 165 505, https://doi.org/10.1016/j.scitotenv.2023.165505, 2023b.

Holm-Hansen, O., Lorenzen, C. J., Holmes, R. W., and Strickland, J. D. H.: Fluorometric Determination of Chlorophyll, ICES Journal of Marine Science, 30, 3–15, https://doi.org/10.1093/icesjms/30.1.3, 1965.

Hubert, Z.: Decennial Automated Observation of Phytoplankton in Marine Surface Waters by the Strait of Dover-Pas de Calais (DYPHYRAD Cruises), in prep.

Huguet, A., Barillé, L., Soudant, D., Petitgas, P., Gohin, F., and Lefebvre, A.: Identifying the Spatial Pattern and the Drivers of the Decline in the Eastern English Channel Chlorophyll-*a* Surface Concentration over the Last Two Decades, Marine Pollution Bulletin, 199, 115 870, https://doi.org/10.1016/j.marpolbul.2023.115870, 2024.

Kendall, M.: Rank Correlation Methods, Rank Correlation Methods, Griffin, Oxford, England, 1948.

Kerr, R. A.: A North Atlantic Climate Pacemaker for the Centuries, Science, 288, 1984–1985, https://doi.org/10.1126/science.288.5473.1984, 2000.

Lamy, D., Obernosterer, I., Laghdass, M., Artigas, L. F., Breton, E., Grattepanche, J. D., Lecuyer, E., Degros, N., Lebaron, P., and Christaki, U.: Temporal Changes of Major Bacterial Groups and Bacterial Heterotrophic Activity during a Phaeocystis Globosa Bloom in the Eastern English Channel, Aquatic Microbial Ecology, 58, 95–107, https://doi.org/10.3354/ame01359, 2009.

Laws, E. A., Falkowski, P. G., Smith Jr., W. O., Ducklow, H., and McCarthy, J. J.: Temperature Effects on Export Production in the Open Ocean, Global Biogeochemical Cycles, 14, 1231–1246, https://doi.org/10.1029/1999GB001229, 2000.

Lefebvre, A. and Devreker, D.: How to Learn More about Hydrological Conditions and Phytoplankton Dynamics and Diversity in the Eastern English Channel and the Southern Bight of the North Sea: The Suivi Régional Des Nutriments Data Set (1992–2021), Earth System Science Data, 15, 1077–1092, https://doi.org/10.5194/essd-15-1077-2023, 2023.

Lefebvre, A., Guiselin, N., Barbet, F., and Artigas, F. L.: Long-Term Hydrological and Phytoplankton Monitoring (1992–2007) of Three Potentially Eutrophic Systems in the Eastern English Channel and the Southern Bight of the North Sea, ICES Journal of Marine Science, 68, 2029–2043, https://doi.org/10.1093/icesjms/fsr149, 2011.

Legendre, P. and Gallagher, E. D.: Ecologically Meaningful Transformations for Ordination of Species Data, Oecologia, 129, 271–280, https://doi.org/10.1007/s004420100716, 2001.

Leynaert, V. R. A., Daoud, N., and Lancelot, C.: Diatom Succession, Silicification and Silicic Acid Availability in Belgian Coastal Waters (Southern North Sea), Marine Ecology Progress Series, 236, 61–73, https://doi.org/10.3354/meps236061, 2002.

Lheureux, A., David, V., Del Amo, Y., Soudant, D., Auby, I., Bozec, Y., Conan, P., Ganthy, F., Grégori, G., Lefebvre, A., Leynart, A., Rimmelin-Maury, P., Souchu, P., Vantrepote, V., Blondel, C., Cariou, T., Crispi, O., Cordier, M.-A., Crouvoisier, M., Duquesne, V., Ferreira, S., Garcia, N., Gouriou, L., Grosteffan, E., Le Merrer, Y., Meteigner, C., Retho, M., Tournaire, M.-P., and Savoye, N.: Trajectories

of Nutrients Concentrations and Ratios in the French Coastal Ecosystems: 20 Years of Changes in Relation with Large-Scale and Local Drivers, Science of The Total Environment, 857, 159 619, https://doi.org/10.1016/j.scitotenv.2022.159619, 2023.

Loebl, M., Colijn, F., van Beusekom, J. E. E., Baretta-Bekker, J. G., Lancelot, C., Philippart, C. J. M., Rousseau, V., and Wiltshire, K. H.: Recent Patterns in Potential Phytoplankton Limitation along the Northwest European Continental Coast, Journal of Sea Research, 61, 34–43, https://doi.org/10.1016/j.seares.2008.10.002, 2009.

Lorenzen, C. J.: Determination of Chlorophyll and Pheo-Pigments: Spectrophotometric Equations, Limnology and Oceanography, 12, 343–346, https://doi.org/10.4319/lo.1967.12.2.0343, 1967.

Louchart, A., Lizon, F., Lefebvre, A., Didry, M., Schmitt, F. G., and Artigas, L. F.: Phytoplankton Distribution from Western to Central English Channel, Revealed by Automated Flow Cytometry during the Summer-Fall Transition, Continental Shelf Research, 195, 104 056, https://doi.org/10.1016/j.csr.2020.104056, 2020.

Louchart, A., Holland, M., Mcquatters-Gollop, A., and Artigas, L. F.: Changes in Plankton Diversity Common Indicator Assessment Changes in Plankton Diversity, in: OSPAR, 2023: The 2023 Quality Status Report for the Northeast Atlantic., p. 38, OSPAR Commission, 2023a.

Louchart, A., Holland, M., Mcquatters-Gollop, A., and Artigas, L. F.: Changes in Phytoplankton Biomass and Zooplankton Abundance Common Indicator Assessment Changes in Phytoplankton Biomass and Zooplankton Abundance, in: OSPAR, 2023: The 2023 Quality Status Report for the Northeast Atlantic., p. 34, OSPAR Commission, 2023b.

Louchart, A., Lizon, F., Debusschere, E., Mortelmans, J., Rijkeboer, M., Crouvoisier, M., Lebourg, E., Deneudt, K., Schmitt, F. G., and Artigas, L. F.: The Importance of Niches in Defining Phytoplankton Functional Beta Diversity during a Spring Bloom, Marine Biology: International Journal on Life in Oceans and Coastal Waters, https://doi.org/10.1007/s00227-023-04346-6, 2024.

Mann, H. B.: Nonparametric Tests against Trend, Econometrica: Journal of the econometric society, pp. 245–259, 1945.

Marañón, E.: Cell Size as a Key Determinant of Phytoplankton Metabolism and Community Structure, Annual Review of Marine Science, 7, 241–264, https://doi.org/10.1146/annurev-marine-010814-015955, 2015.

Margalef, R.: Life-Forms of Phytoplankton as Survival Alternatives in an Unstable Environment, Oceanologica acta, 1, 493–509, 1978.

Marrec, P., Sammari, C., Ben Ismail, A., Ben Ismail, S., Grégori, G., Denis, M., Lahbib, S., and Thyssen, M.: Dynamics of the Phytoplankton Community Structure in the Western Mediterranean Sea Using Automated Flow Cytometry on a Voluntary Observing Ship during Fall/Winter., in: ASLO 2021, on-line, France, 2021.

Masselink, G., Scott, T., Poate, T., Russell, P., Davidson, M., and Conley, D.: The Extreme 2013/2014 Winter Storms: Hydrodynamic Forcing and Coastal Response along the Southwest Coast of England, Earth Surface Processes and Landforms, 41, 378–391, https://doi.org/10.1002/esp.3836, 2016.

Matthews, T., Murphy, C., Wilby, R. L., and Harrigan, S.: Stormiest Winter on Record for Ireland and UK, Nature Climate Change, 4, 738–740, https://doi.org/10.1038/nclimate2336, 2014.

McLean, M. J., Mouillot, D., Goascoz, N., Schlaich, I., and Auber, A.: Functional Reorganization of Marine Fish Nurseries under Climate Warming, Global Change Biology, 25, 660–674, https://doi.org/10.1111/gcb.14501, 2019.

McQuatters-Gollop, A., Stern, R. F., Atkinson, A., Best, M., Bresnan, E., Creach, V., Devlin, M., Holland, M., Ostle, C., Schmidt, K., Sheppard, L., Tarran, G., Woodward, E. M. S., and Tett, P.: The Silent Majority: Pico- and Nanoplankton as Ecosystem Health Indicators for Marine Policy, Ecological Indicators, 159, 111 650, https://doi.org/10.1016/j.ecolind.2024.111650, 2024.

Mehner, T., Lischke, B., Scharnweber, K., Attermeyer, K., Brothers, S., Gaedke, U., Hilt, S., and Brucet, S.: Empirical Correspondence between Trophic Transfer Efficiency in Freshwater Food Webs and the Slope of Their Size Spectra, Ecology, 99, 1463–1472, https://doi.org/10.1002/ecy.2347, 2018.

Pannard, A., Claquin, P., Klein, C., Roy, B., and Véron, B.: Short-Term Variability of the Phytoplankton Community in Coastal Ecosystem in Response to Physical and Chemical Conditions' Changes, Estuarine Coastal and Shelf Science, 80, 212–224, https://doi.org/10.1016/j.ecss.2008.08.008, 2008.

Peter, K. H. and Sommer, U.: Phytoplankton Cell Size Reduction in Response to Warming Mediated by Nutrient Limitation, PLOS ONE, 8, e71 528, https://doi.org/10.1371/journal.pone.0071528, 2013.

Pörtner, H.-O., Roberts, D., Tignor, M., Poloczanska, E., Mintenbeck, K., Alegria, A., Craig, M., Langsdorf, S., Löschke, S., Möller, V., Okem, A., and Rama, B., eds.: Climate Change 2022: Impacts, Adaptation and Vulnerability. Contribution of Working Group II to the Sixth Assessment Report of the Intergovernmental Panel on Climate Change, Cambridge University Press, Cambridge University Press, Cambridge, UK and New York, NY, USA, cambridge university press edn., 2022.

Redfield, A. C., Ketchum, B. H., and Richards, F. A.: The Influence of Organisms on the Composition of Seawater, The sea, 2, 26–77, 1963.

Regier, P., Briceño, H., and Boyer, J. N.: Analyzing and Comparing Complex Environmental Time Series Using a Cumulative Sums Approach, MethodsX, 6, 779–787, https://doi.org/10.1016/j.mex.2019.03.014, 2019.

Richardson, A. J. and Schoeman, D. S.: Climate Impact on Plankton Ecosystems in the Northeast Atlantic, Science, 305, 1609–1612, https://doi.org/10.1126/science.1100958, 2004.

Robache, K.: Phytoplankton Dynamics in a Coastal System of the Eastern English Channel: The Boulogne-sur-Mer Harbour, in prep.

Rombouts, I., Simon, N., Aubert, A., Cariou, T., Feunteun, E., Guérin, L., Hoebeke, M., McQuatters-Gollop, A., Rigaut-Jalabert, F., and Artigas, L. F.: Changes in Marine Phytoplankton Diversity: Assessment under the Marine Strategy Framework Directive, Ecological Indicators, 102, 265–277, https://doi.org/10.1016/j.ecolind.2019.02.009, 2019.

Saulquin, B. and Gohin, F.: Mean Seasonal Cycle and Evolution of the Sea Surface Temperature from Satellite and in Situ Data in the English Channel for the Period 1986–2006, International Journal of Remote Sensing, 31, 4069–4093, https://doi.org/10.1080/01431160903199155, 2010.

Schapira, M., Vincent, D., Gentilhomme, V., and Seuront, L.: Temporal Patterns of Phytoplankton Assemblages, Size Spectra and Diversity during the Wane of a Phaeocystis Globosa Spring Bloom in Hydrologically Contrasted Coastal Waters, Journal of the Marine Biological Association of the United Kingdom, 88, 649–662, https://doi.org/10.1017/S0025315408001306, 2008.

Schmidt, K., Birchill, A. J., Atkinson, A., Brewin, R. J. W., Clark, J. R., Hickman, A. E., Johns, D. G., Lohan, M. C., Milne, A., Pardo, S., Polimene, L., Smyth, T. J., Tarran, G. A., Widdicombe, C. E., Woodward, E. M. S., and Ussher, S. J.: Increasing Picocyanobacteria Success in Shelf Waters Contributes to Long-Term Food Web Degradation, Global Change Biology, 26, 5574–5587, https://doi.org/10.1111/gcb.15161, 2020.

Scholz, S. R., Seager, R., Ting, M., Kushnir, Y., Smerdon, J. E., Cook, B. I., Cook, E. R., and Baek, S. H.: Changing Hydroclimate Dynamics and the 19th to 20th Century Wetting Trend in the English Channel Region of Northwest Europe, Climate Dynamics, 58, 1539–1553, https://doi.org/10.1007/s00382-021-05977-5, 2022.

Sen, P. K.: Estimates of the Regression Coefficient Based on Kendall's Tau, Journal of the American Statistical Association, 63, 1379–1389, https://doi.org/10.1080/01621459.1968.10480934, 1968.

Sentchev, A. and Yaremchuk, M.: VHF Radar Observations of Surface Currents off the Northern Opal Coast in the Eastern English Channel, Continental Shelf Research, 27, 2449–2464, https://doi.org/10.1016/j.csr.2007.06.010, 2007.

Shapiro, S. S. and Wilk, M. B.: An Analysis of Variance Test for Normality (Complete Samples), Biometrika, 52, 591–611, https://doi.org/10.2307/2333709, 1965.

Simon, A., Poppeschi, C., Plecha, S., Charria, G., and Russo, A.: Coastal and Regional Marine Heatwaves and Cold Spells in the Northeastern Atlantic, Ocean Science, 19, 1339–1355, https://doi.org/10.5194/os-19-1339-2023, 2023.

Simon, N., Cras, A.-L., Foulon, E., and Lemée, R.: Diversity and Evolution of Marine Phytoplankton, Comptes Rendus Biologies, 332, 159–170, https://doi.org/10.1016/j.crvi.2008.09.009, 2009.

Sommer, U. and Lengfellner, K.: Climate Change and the Timing, Magnitude, and Composition of the Phytoplankton Spring Bloom, Global Change Biology, 14, 1199–1208, https://doi.org/10.1111/j.1365-2486.2008.01571.x, 2008.

Sommer, U., Charalampous, E., Genitsaris, S., and Moustaka-Gouni, M.: Benefits, Costs and Taxonomic Distribution of Marine Phytoplankton Body Size, Journal of Plankton Research, 39, 494–508, https://doi.org/10.1093/plankt/fbw071, 2017a.

Sommer, U., Peter, K. H., Genitsaris, S., and Moustaka-Gouni, M.: Do Marine Phytoplankton Follow Bergmann's Rule Sensu Lato?, Biological Reviews, 92, 1011–1026, https://doi.org/10.1111/brv.12266, 2017b.

Talarmin, A., Lomas, M. W., Bozec, Y., Savoye, N., Frigstad, H., Karl, D. M., and Martiny, A. C.: Seasonal and Long-Term Changes in Elemental Concentrations and Ratios of Marine Particulate Organic Matter, Global Biogeochemical Cycles, 30, 1699–1711, https://doi.org/10.1002/2016GB005409, 2016.

Thyssen, M., Grégori, G. J., Grisoni, J.-M., Pedrotti, M. L., Mousseau, L., Artigas, L. F., Marro, S., Garcia, N., Passafiume, O., and Denis, M. J.: Onset of the Spring Bloom in the Northwestern Mediterranean Sea: Influence of Environmental Pulse Events on the in Situ Hourly-Scale Dynamics of the Phytoplankton Community Structure, Frontiers in Microbiology, 5, https://doi.org/10.3389/fmicb.2014.00387, 2014.

Thyssen, M., Grégori, G., Créach, V., Lahbib, S., Dugenne, M., Aardema, H. M., Artigas, L.-F., Huang, B., Barani, A., Beaugeard, L., Bellaaj-Zouari, A., Beran, A., Casotti, R., Del Amo, Y., Denis, M., Dubelaar, G. B. J., Endres, S., Haraguchi, L., Karlson, B., Lambert, C., Louchart, A., Marie, D., Moncoiffé, G., Pecqueur, D., Ribalet, F., Rijkeboer, M., Silovic, T., Silva, R., Marro, S., Sosik, H. M., Sourisseau, M., Tarran, G., Van Oostende, N., Zhao, L., and Zheng, S.: Interoperable Vocabulary for Marine Microbial Flow Cytometry, Frontiers in Marine Science, 9, https://doi.org/10.3389/fmars.2022.975877, 2022.

Tinker, J., Howes, E., Wakelin, S., Menary, M., Kent, E., Berry, D. I., Hindson, J., Ribeiro, J., Dye, S., Andres, O., Lyons, K., and Smyth, T.: The Impacts of Climate Change on Temperature (Air and Sea), Relevant to the Coastal and Marine Environment around the UK, in: MCCIP Science Review 2020, pp. 1–30, Marine Climate Change Impacts Partnership, 2020.

Tukey, J. W.: Comparing Individual Means in the Analysis of Variance, Biometrics, 5, 99–114, https://doi.org/10.2307/3001913, 1949.

Vigiak, O., Udías, A., Grizzetti, B., Zanni, M., Aloe, A., Weiss, F., Hristov, J., Bisselink, B., de Roo, A., and Pistocchi, A.: Recent Regional Changes in Nutrient Fluxes of European Surface Waters, Science of The Total Environment, 858, 160 063, https://doi.org/10.1016/j.scitotenv.2022.160063, 2023.

Winder, M. and Sommer, U.: Phytoplankton Response to a Changing Climate, Hydrobiologia, 698, 5–16, https://doi.org/10.1007/s10750-012-1149-2, 2012.

Wu, Y., Wen, Y., Zhou, J., and Wu, Y.: Phosphorus Release from Lake Sediments: Effects of pH, Temperature and Dissolved Oxygen, KSCE Journal of Civil Engineering, 18, 323–329, https://doi.org/10.1007/s12205-014-0192-0, 2014.

Zohary, T., Fishbein, T., Shlichter, M., and Naselli-Flores, L.: Larger Cell or Colony Size in Winter, Smaller in Summer – a Pattern Shared by Many Species of Lake Kinneret Phytoplankton, Inland Waters, 7, 200–209, https://doi.org/10.1080/20442041.2017.1320505, 2017.

Zohary, T., Flaim, G., and Sommer, U.: Temperature and the Size of Freshwater Phytoplankton, Hydrobiologia, 848, 143–155, https://doi.org/10.1007/s10750-020-04246-6, 2021.